# Studies on the Molecular Mechanisms of the Bystander Effect in HSV-TK mediated Suicide Gene Therapy for Glioblastoma Treatment

**Sayintha Jeyendran**

This thesis is submitted in partial fulfilment of the requirements for the degree of Master in Biomedical Sciences

Department of Biomedicine, Faculty of Medicine

University of Bergen

Spring 2020

# Acknowledgements

If you had asked me two years ago, I would never have guessed that I would handing in this thesis in the midst of a worldwide pandemic. The past two years have been educational and challenging, and there are several people whom I would especially like to thank for believing in me.

I would first like to express my gratitude to my supervisors, Prof. Hrvoje Miletic and Jubayer Hossain for giving me the opportunity to be a part of the Miletic Research Lab and for introducing me to suicide gene therapy- a promising therapy for glioblastoma treatment. I am very grateful for your guidance, unending support and feedbacks throughout the course of my Masters.

I would also like to thank all the colleges of Translational Cancer Research group- especially, the technical staff for always being so approachable, postdoctoral fellow Taral R. Lunavat for sharing your expertise, techniques and inputs within the field of extracellular vesicles and Romi Roy Choudhury for being helpful in the lab. My thanks is also to be reached out to Endy Spirit (Molecular Imaging Centre) and Even Birkeland (PROBE department) for supporting me with important results in this thesis.

I am also very grateful for my office friends and co-graduate students, especially, Emma, Dayne, Mina, Anders, Stefan, Christer, Johannes, Ege and Lars for your encouragement, support and laughter during tough times.

Lastly, I am deeply grateful to my dad, mom, three sisters, brother in law, closest family and childhood friends for your endless support, love and for always believing in me despite the distance. Great thanks to my second family and friends in Bergen for always being supportive, but especially for being my home away from home.

Thank you to all of you for being an important part of my research life and for encouraging me to be a better scientist.

Sayintha Jeyendran

Bergen, June 2020

# Table of contents

# Abbreviations

**5-FC** 5-fluorocytosine
**ApoBD** Apoptotic bodies
**BE** Bystander Effect
**CD** Cytosine deaminase
**CNS** Central Nervous System
**DMEM** Dulbecco's Modified Eagle's Medium
**DMSO** Dimethyl Sulfoxide
**EGFR** Epidermal Growth Factor Receptor
**EXOS** Exosomes
**FBS** Fetal Bovine Serum
**EVs** Extracellular vesicles
**g** Gram
**GBM** Glioblastoma
**GCV** Ganciclovir
**GCV-MP** Ganciclovir Monophosphate
**GCV-TP** Ganciclovir -Triphosphate
**HCMV** Human Cytomegalovirus
**HIF** Hypoxia Inducible Factor
**HRP** Horseradish Peroxidase
**HSV-TK** Herpes Simplex Virus Thymidine Kinase
**IDH1** Isocitrate Dehydrogenase I
**IL-8** Interleukin-8
**ISEV** International Society for Extracellular Vesicle
**κB** Nuclear factor
**LOH** Loss of Heterozygosity
**LFS** Li Fraumeni syndrome
**MS** Mass spectrometry
**MGMT** Methylguanine DNA Methyltransferase
**MHC** Major histocompatibility complex
**MES** Mesenchymal
**MISEV** Minimal Information for Studies of Extracellular Vesicles
**MVBs** Multi-vesicular bodies
**MVs** Microvesicles
**NBM** Neurobasal Medium

**NEAA** Non-essential amino acids

**NF1** Neurofibromatosis type-1

**PBS** Phosphate-Buffered Saline

**PN** Proneural

**PTEN** Phosphate and Tension Homolog on Chromosome 10

**PI3K** Phosphatidyl inositol 3.4.5 biphosphate kinase

**PDFGR** Platelet Derived Growth Factor Receptor

**RIPA** Radradioimmunoassay precipitation buffer

**RT** Radiotherapy

**RTK** Receptor Tyrosine Kinase

**SDS** Sodium Dodecyl Sulfate

**SDS-PAGE** Sodium Dodecyl Polyacrylamide Gel Electrophoresis

**SGT** Suicide Gene Therapy

**TBS-T** Tris Buffered Saline-Tween 20

**TEM** Transmission electron microscopy

**TEMED** Tetramethylethylenediamine

**TK** Thymidine Kinase

**TMZ** Temozolomide

**TP53** Tumor Protein 53

**VEGF** Vascular Endothelial Growth Factor

**VHL** von Hippel-Lindau

**WHO** World Health Organization

**WST** Water Soluble Tetrazolium

# List of Figures

# List of Tables

# Summary

Glioblastoma (GBM) is the most common and most malignant primary brain tumor. The highly invasive nature of GBM limits the outcome of standard therapy. The resistance to conventional therapy, including safe surgical resection, followed by radiotherapy (RT) and chemotherapy, leads to a poor median survival of 14.6 months after diagnosis. The highly immunosuppressive microenvironment and tumor heterogeneity make it difficult to treat GBM. Thus, new and more innovative treatment strategies are urgently needed to improve the poor prognosis of GBM patients. In this regard, several molecular targeted therapies have been developed and tested over the last two decades. Gene therapy is one of the new promising strategies that may improve patient outcome.

Herpes simplex virus thymidine kinase gene (HSV-TK)/Ganciclovir (GCV) suicide gene therapy (SGT) converts a nontoxic prodrug into a cytotoxic drug that kills dividing tumor cells. It has been shown in earlier studies that the metabolized cytotoxic drug spreads to neighboring cells through gap junctions to execute the so-called bystander effect (BE). This phenomenon is highly important for SGT as the transduction of 100% tumor cells in a given tumor is impossible, even with highly efficient viral vectors. While gap junction-mediated BE is highly characterized in the HSV-TK/GCV system, it is not clear if soluble factors such as apoptotic bodies (ApoBDs), microvesicles (MVs) and exosomes (exo) play any role in this process.

In this project we investigated the potential involvement of these soluble cellular factors in the process of HSV-TK/GCV-mediated BE. We hypothesized that GCV treatment of tumor cells would increase the secretion of extracellular vesicles (EVs) and thus contribute to an increased BE. Two alternative mechanisms could contribute to this BE, either by loading of EVs with the HSV-TK.GFP protein or with GCV. Here, we focused on investigating the presence of the protein in EVs.

In this present study, we used the human U87 glioma cell line to investigate the increase of EV-secretion following HSV-TK/GCV gene therapy, which could in theory contribute to BE. Our study showed successful secretion and harvest of EVs in this model system. We were also able to show EV secretion in the patient-derived glioblastoma P3 cell line cultured in serum-free neurobasal medium, which is more relevant to the clinical scenario. Most importantly, we showed for the first time the

presence of the TK.GFP protein in ApoBDs, MVs and exosomes derived from TK-containing cells.

In conclusion, our study highlights that the TK protein can be loaded in EVs secreted from TK-expressing cells. Thus, the transfer of the TK protein through EVs might be an important contributor to the BE in SGT. In the future it will be important to investigate if also TK mRNA is transferred through EVs and then translated into active protein in the recipient cells and/or if transfer of phosphorylated GCV can contribute to EV-mediated BE.

# 1. Introduction

## 1.1 Cancer

Cancer is referred to a group of diseases characterized by uncontrolled cell growth and proliferation [1]. In a seminal paper Hanahan and Weinberg proposed six key hallmarks of cancer namely: Evading growth supressors, activating invasion and metastasis, enabling replicative immortality, inducing angiogensis, resisting cell detah and sustaining prolifertaive signaling [2]. Self-sufficiency of growth signals and insensitivity to anti-growth signals leads to unregulated growth and accumulation of mutations. These acquired and inherited unfavorable abnormalities result in tumor formation. Metastasis, the process that refers to colonization of tumor cells from the tissue of origin to a distant tissue, is the primary cause of cancer morbidity and mortality [3]. Although most tumors harbor genetic abnormalities in some common set of signalling pathways, tumorigenesis is very complex, and the underlying cellular and molecular pathways may vary within different cancer types [3]. Extensive research over the last decade has identified more biological processes associated with carcinogenesis. In line, Hanahan and Weinberg lately introduced two more enabling hallmarks; tumor promoting inflammation and genome instability [2].

## 1.2 Brain cancer

Tumors are classified into two main groups: benign or malignant tumors [4]. Neoplastic growth of cells in the brain or central nervous system (CNS) leads to tumor formation. When the origin of neoplastic growth is located inside the brain, the corresponding tumors are called primary brain tumors. When malignant tumors originate in other body parts and metastasize to the brain, the tumors are called secondary brain tumors. Most common sites of origin of secondary brain tumors are skin, colon, lungs or breast [5]. As the present work is based on primary brain tumors, this tumor class will be described in more detail. The most common form of primary brain tumors are collectively known as gliomas. This assembly of tumors is based on the hypothesized cellular root of the individual entities- the glial cell [6]. The term glioma was coined by Dr. Rudolph Virchow in 1860 [7] , who also discovered and named the glial cells (glue in Greek) in 1854.

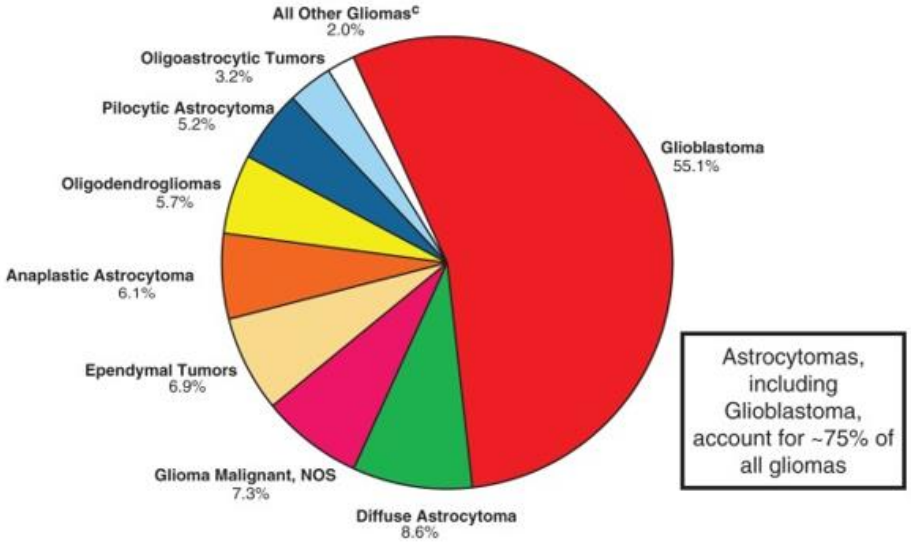


**Figure 1.1. Pie chart showing the distribution of different gliomas by histological subtypes in the USA.** Astrocytoma including Glioblastoma acount for ~ 75% of all gliomas. This distribution is from 2008-2012, n= 97.910. Figure is adopted from [8]

Astrocytomas, account for 75% of all "nondiffuse" gliomas, and they are the most frequent and malignant representative. These subgroups are assigned with malignancy grade (WHO grade I, II, III or IV) based on the appearance/nonappearance of mitotic activity, microvascular proliferation and necrosis[9]

Classification of Astrocytoma

- Grade I astrocytoma (Pilocytic astrocytoma): Benign and non-infiltrating tumor. It is characterized by slow growth rate without any nuclear atypia [10].
- Grade II astrocytoma (Low-grade/diffuse astrocytoma): Shows no sign of malignancy and express moderate nuclear atypia [11].
- Grade III astrocytoma (Anaplastic astrocytoma): Characterized by nuclear atypia, lacking necrosis and increased cellularity [12].
- Grade IV astrocytoma (Glioblastoma): The most malignant astrocytoma with presence of microvascular proliferation and necrosis.

Grade I astrocytoma (low-grade) is most seen in children and young adults. The tumors are less clinically aggressive and often removed by surgery alone. Grade II-IV poses a difficulty for treatment and normally requires combination therapy that involves surgical resection of the tumor followed by temozolomide (TMZ) chemotherapy and radiotherapy [13].

## 1.3 Glioblastoma (GBM)

GBM is the most common type of glioma. GBM patients have a median survival time of about 15 months after diagnosis making it one of the most aggressive cancers in humans [13]. The incididence rate of GBM is 2-3 new cases per 100 000 people among adults in Europe and North America and it is slightly higher in men compared to women (1.26:1) [14]. GBM cases in children and infants are less frequent and although no morphological differences are observed compared to adult GBMs, pediatric GBMs have a completely different mutational profile [14]. Although GBM is sporadic, underlying rare genetic disorders such as Turcot syndrome, multiple endocrine neoplasia type IIA, tuberous sclerosis, neurofibromatosis type-1 (NF1) and Li Fraumeni syndrome (LFS) are associated with GBM incidents [14, 15]. Some epidemiology studies also support the link between traumatic brain injury and subsequent GBM formation [16, 17]. Higher incidence of GBM in Caucasians and especially people living close to industrial areas have also been reported [18]. Certain viruses, such as human cytomegalovirus (HCMV) have also been reported to have an impact on GBM development [14]. Pesticides, polycyclic aromatic compounds and other solvents that are considered as dangerous chemicals can increase the likelihood for developing GBM, as well as ionizing radiation [14, 18]. Genetically and phenotypically GBM consist of heterogenous group of tumors which are histologically indistinguishable. Although no morphological differences have been observed, GBM is divided into two subgroups due to different genetic mechanisms and pathways of tumorigenesis: primary GBM and secondary GBM [19]. Primary GBM develop rapidly *de novo* in elderly people without any signs of a lower grade precursor lesion and it accounts for ~90% of all GBMs. In contrast, secondary GBM have a delayed development through progression from low-grade astrocytoma or anaplastic astrocytoma. Secondary GBM has a higher incidence in younger patients, but it accounts for the minority of total GBM cases [20].

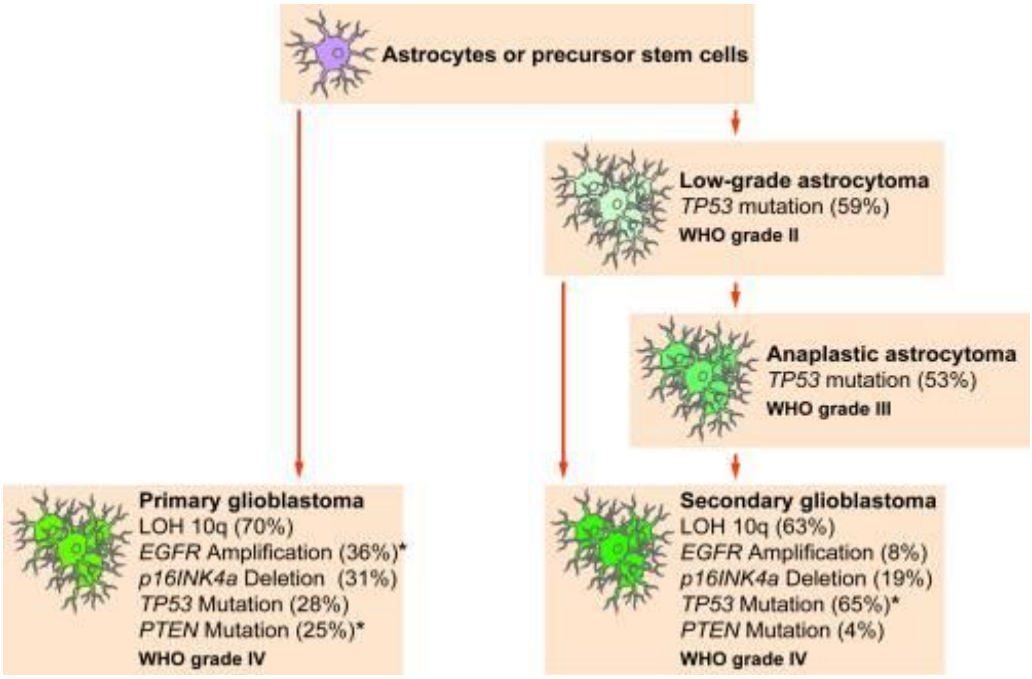


**Figure 1.2 Primary and Secondary GBMs.** Primary GBM develop rapidly *de novo* and accounts for ~ 90% of all gliomas. Secondary GBM have a delayed development through progression from low-grade astrocytoma and accounts for the minority of all GBM cases. Figure is adapted from [20].

Primary GBM is characterized by gain of chromosome 7 and by amplification/overexpression and mutations of Epidermal Growth Factor Receptor (EGFR). Deletion of tumor suppressor phosphatase and tension homolog on chromosome 10 (PTEN) and 16q [19, 20] are also frequently observed. PTEN functions as a cellular phosphatase and in case of inactivating mutation results in a constitutively activated Phosphatidylinositol 3.4.5 biphosphate kinase (PI3K/Akt) pathway. Isocitrate Dehydrogenase I (IDHI) is an enzyme that has an important role in energy metabolism and mutation in this component is related to the occurrence of glioma [21]. Although, IDH1 mutations are rarely seen in primary GBM (<5%), they are represented in a much higher degree in secondary GBM (>80%) and also low grade gliomas [22]. Loss of heterozygosity (LOH) on chromosome arm 10q is the most frequent genetic alteration seen in both primary and secondary GBMs.

Based on gene expression and mRNA profiling GBM is subclassified into proneural (PN), mesenchymal (MES) and classical GBMs, each with different pattern of disease and survival outcomes [23] . The PN subtype is associated with IDH1 mutations, Platelet-Derived Growth factor receptor (PDGFR) amplification/mutation and Tumor protein 53 (TP53) [24], while EGFR amplification is characteristic for the classical

subtype. The mesenchymal subtype often harbours *NF1* mutations and shows strong activation of the Nuclear factor-κB (NF- κB) pathway [23]. NF- κB consists of a family of transcription factors that is highly involved in inflammation, survival, differentiation, immunity and cell proliferation [25]. Thus, it is not surprising that mesenchymal GBM consist of an inflammatory tumor microenvironment which is dominated by immunosuppressive macrophages/microglia. The mesenchymal subtype is also associated with the poorest prognosis and the worst patient outcome [23].

### 1.4 Histopathological features of GBM

As the name "multiforme" suggest, the histopathological features of GBM are many and various in its appearance. As described previously (section 1.2), GBM is composed of a pleomorphic tumor cell population showing nuclear atypia and mitotic activity. In addition, microvascular proliferation and necrotic areas are specific for GBMs and are usually not observed in low grade gliomas. The formation of pseudopalisading necrotic regions is a result of cells escaping the hypoxic and necrotic areas which are characterized by oxygen and nutrition depletion [26, 27]. Pseudopalisading cells show increased expression of hypoxia-inducible factor (HIF) which leads to secretion of the HIF target gene vascular endothelial growth factor (VEGF) at high levels. Together with Interleukin-8 (IL-8), this reaction stimulates an excessive angiogenic response.

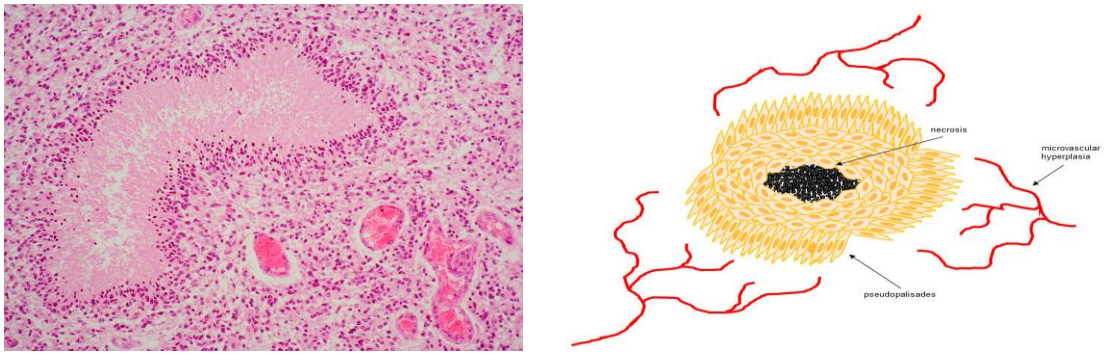


**Figure 1.3. Palisading of tumor cells and microvascular proliferation around necrosis.** Left figure adapted from [28]. Right figure adapted from [29]

## 1.5 Current treatments for GBM

As described earlier, GBM is a primary brain tumor with a remarkably poor prognosis. 1/3 of the patients dies of the disease within a year after diagnosis. The standard therapy for GBM treatment is maximal neurosurgical resection followed by radiotherapy and adjuvant concomitant chemotherapy with temozolomide (TMZ) [14]. Complete resection of the tumor is not feasible due to its extreme invasive nature and capability to infiltrate surrounding healthy brain tissue. Surgery is therefore followed by radiotherapy (RT) to eliminate the remaining tumor cells. As a result of radiation, the DNA damage response pathway is induced in the proliferative tumor cells [30, 31]. Until 2005 the standard treatment of care for GBM was resection of the tumor followed by only RT. However, Stupp et al. showed that the combination of RT with concurrent TMZ chemotherapy was more effective than RT alone. Patients receiving both RT and TMZ had an increased median survival of 14.6 months compared to 12.1 months with RT only [30]. TMZ is an orally-given alkylating anti-cancer agent that functions by breaking DNA-double strands, subsequently causing cell cycle arrest and ultimately cell death [32]. The success of TMZ treatment is affected by the methylation of $O^6$-Methylguanine DNA methyltransferase (MGMT), which is a DNA repair enzyme. A methylated MGMT enhances DNA damage in tumor cells upon TMZ treatment that results in apoptosis and cytotoxicity and thus improves patient outcome [32, 33]. Despite the improvement of standard treatment, most GBM patients experience recurrences within 6 months following TMZ discontinuation [34]. Additionally, tumor cells can become resistant to the effect of TMZ.

Thus, new and more innovative treatment strategies are urgently needed to improve the poor prognosis of GBM patients. To improve the treatment modality further, over the last two decades several molecular targeted therapies have been developed and tested. Figure 1.4 shows the overview of the therapies that fell short of expectation in terms of therapeutic efficacy [35]. Gene therapy is one of the new promising strategies that can overcome these obstacles and will be introduced in the next section.

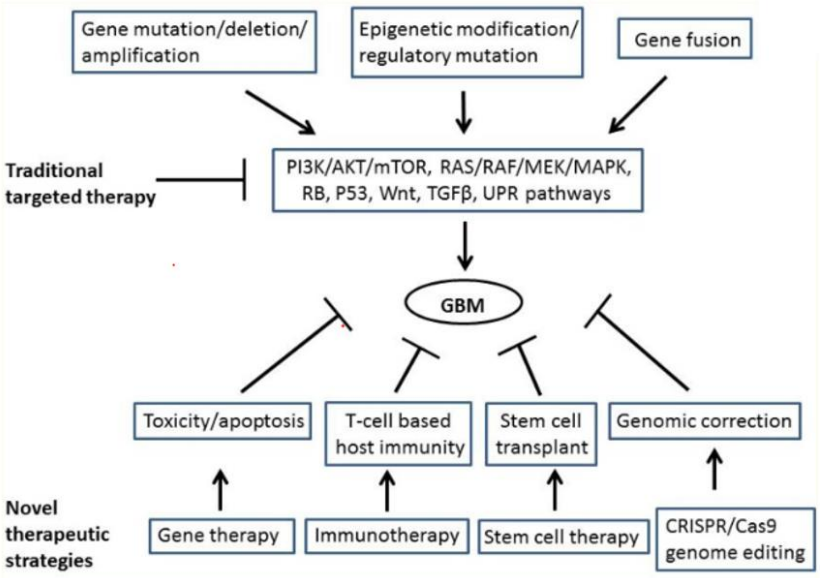


**Figure 1.4 Traditional targeted therapy vs. Novel therapeutic strategies.** Traditional therapy hindered by BBB and the heterogenic nature of tumor cells. Novel therapeutic approaches are promising for the future. Figure is adapted from [36]

## 1.6 Gene therapy

Scientist have been working for decades on multiple ways to manipulate the human genome since the recognition of the gene as the basic unit of heredity. Gene therapy is defined as strategies involving modification of genes or replacement of abnormal or altered genes with healthy ones to prevent, treat or cure a disease or a medical condition [37]. Initially, gene therapy was conceived to treat genetic diseases by substituting one single mutated gene through delivery of a functional version of the gene. This idea was further developed to include the delivery of engineered genetic material to target cancer cells by killing or enhance the immune response against them [38]. Applying gene therapy for cancer has been challenging as tumors develop through multiple known and unknown genetic abnormalities and it requires replacement of several genes. Strategies for cancer, gliomas in particular, has been in development for several decades, and major approaches have been employed for gene therapy of GBM. This includes delivery of suicide genes, cytokine genes, tumor-suppressor genes [38, 39]. Different carriers of the genetic material have been developed. Viruses are evolved as effective vehicles for horizontal gene transfer as they efficiently target mammalian cells. Thus, viruses are the preferred type of vector for gene therapy approaches. Other agents such as stem cells, nanoparticles and

liposomes have also been developed. Cellular carriers such as neural, mesenchymal or embryonic stem cells can additionally be used due to their competence to spread within the tumor tissue and migrate to distant tumor areas [40].

Different approaches for gene therapy have been developed for GBM treatment. Major approaches used for gene therapy against GBM include suicide gene therapy, oncolytic gene therapy, cytokine mediated gene therapy, and tumor suppressor gene therapy [40, 41].

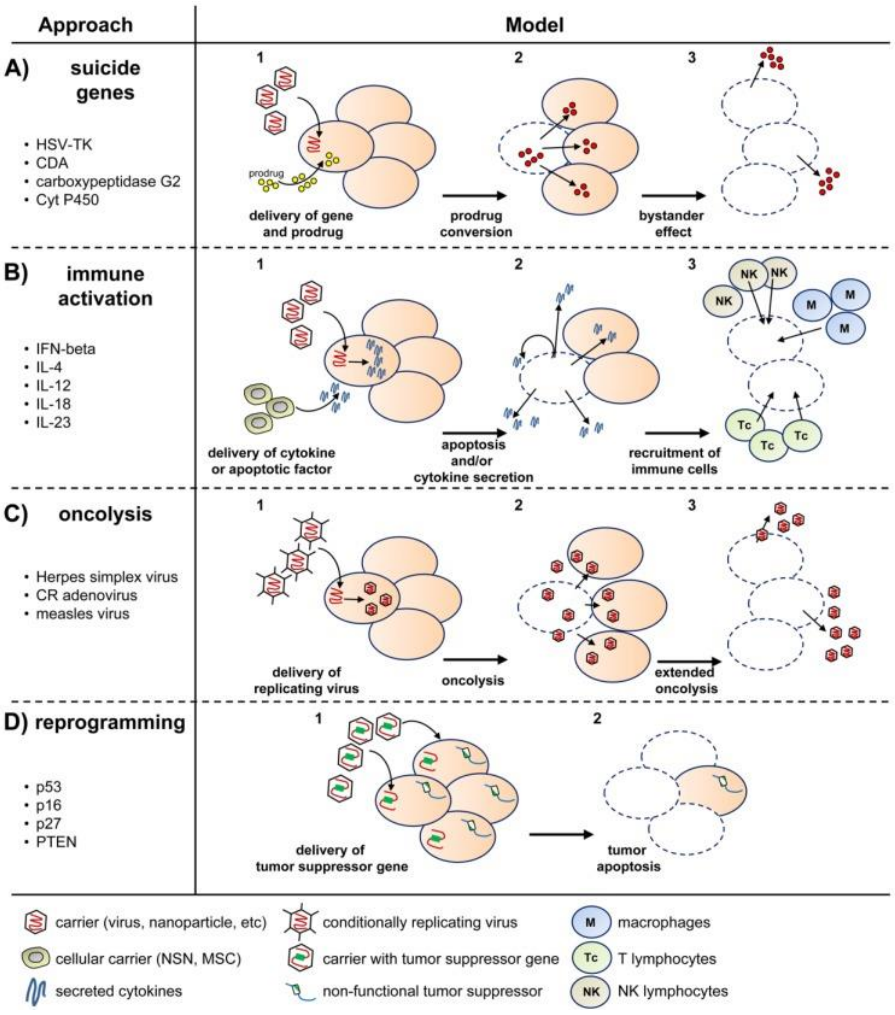


**Figure 1.5 Different Gene therapy approaches of GBM.** A) Suicide genes: Prodrug is converted into a cytotxic drug upon delivery of the suicide gene and kills recipeient cells and surrounding tumor cells. B) Immune activation: Immune cells attracted to tumor cells upon delivery of cytokine genes. C) Oncolysis: Conditionally-replicating oncolytic viruses lyse the tumor cellsupon infection and replication. D) Reprogramming: Tumor cells are reprogrammed by delivery of a functional copy of a tumor supressor gene that induce celle cycle arrest or apoptosis. Figure adapted from [38].

### 1.6.1 Suicide gene therapy and HSV-TK/GCV system

SGT is a therapeutic strategy that is based on the conversion of a prodrug into a toxic drug by transgenes [42]. A prodrug is an inactive compound that after administration is metabolized into a pharmacologically active drug [43]. This system involves the transduction of cancer cells with a recombinant genetic segment (known as the suicide gene) encoding an enzyme. That particular enzyme is responsible for catalyzing the non-toxic prodrug into a cytotoxic drug [44].

Various suicide gene therapy systems have been developed and the two major systems currently being pursued are the herpes simplex virus thymidine kinase gene (HSV-TK) with ganciclovir (GCV) as prodrug and cytosine deaminase (CD) of *Escherichia coli* with non-toxic 5-fluorcytosine (5-FC) as prodrug [43]. The HSV-TK gene metabolizes GCV to ganciclovir monophosphate (GCV-MP). GCV-MP is further phosphorylated into the cytotoxic ganciclovir-trisphosphate (GCV-TP) by the action of different cellular kinases [45]. Cellular enzymes are presented in all cells, but suicide enzymes are selectively transduced/activated in the tumor cells via gene therapy. GCV-TP acts as a nucleoside analog and gets incorporated into the DNA of dividing cells. This results in DNA damage, subsequent cell cycle arrest followed by apoptosis. Normal dividing cells are not affected by the toxicity as the analogs are not efficiently recognized by the wild type enzymes [46].

Several tumor models revealed powerful killing by the HSV-TK/GCV system. However, the killing efficacy is increased with the recombinant version of HSV-TK, termed TK.007, when compared to wild type HSV-TK [47, 48]. In order to obtain positive therapeutic outcome, the selection of the viral vector for gene delivery is essential. Lentiviral vectors are competent of integrating into the genome of both dividing and non-dividing cells, which makes them appealing in brain tumor gene therapy

## 1.7 Bystander effect

The efficiency of SGT largely depends on a phenomenon called bystander effect (BE) whereby the transduced cancer cells transfer the already-metabolized drug to the untransduced cells. As a result, the untransduced cancer cells also undergo cell death [49]. Thus, a potent bystander effect is crucial to induce therapeutic efficacy, because

gene transfer remains to be a limiting factor for suicide gene therapy even with highly optimized vector systems [50]. Thus, in principle, only a fraction of tumor cells need to express HSV-TK to obtain a large killing effect after GCV administration [51]. GCV-TP, the final toxic metabolite is not able to diffuse through cellular membrane to neighboring cells to execute the BE. Initially, it was suggested that the BE was promoted through a mechanism involving cell-to-cell contact. Later, it was indicated that phosphorylated GCV was actively transported through gap junctional intracellular communication from TK positive cells to negative cells [49].

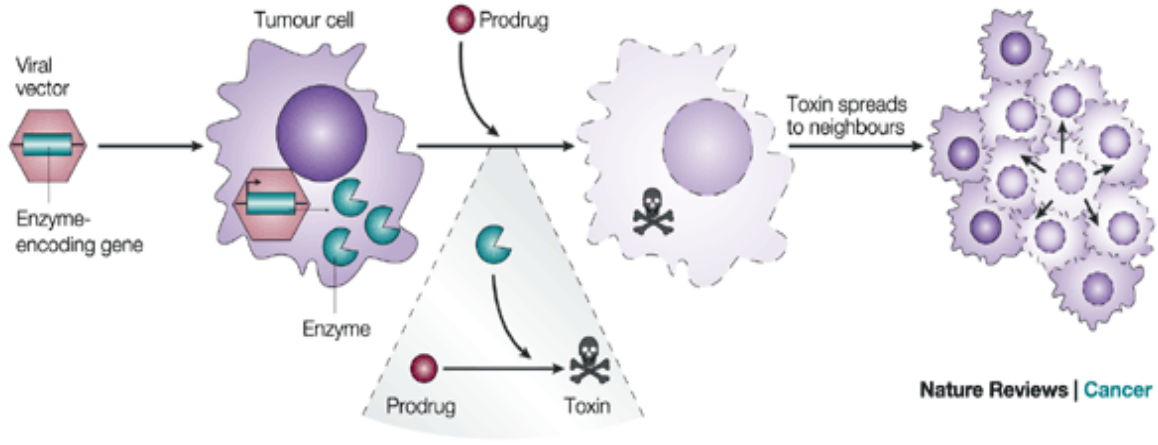


**Figure 1.6: Suicide Gene Therapy.** Bystander effect is executed on neighboring tumor cells when the non-toxic prodrug is metabolized into toxic drug upon suicide gene delivery into the tumor. Figure is adapted from [52].

Gap junctions are a cluster of channels composed of membrane proteins that allows for intracellular communication between adjacent cells via diffusion of ions and small molecules [53, 54]. Six connexin proteins together oligomerize into a connexon at the cell surface. Connected connexons of two adjacent cells ensure for gap junction-mediated intracellular communication [55]. The primary mechanism of the BE *in vitro* has been attributed to connexin 43-mediated gap junction communication, however the expression of connexins *in vivo* is more heterogenous which might affect the efficiency of HSV-TK/GCV therapy.

While gap junction-mediated BE is highly characterized in the HSV-TK/GCV system, it is not properly clear if vesicles secreted from the tumor cells such as apoptotic bodies (ApoBDs), microvesicles (MVs) and exosomes (Exo) play any role in this

process. ApoBD-mediated BE was reported in murine sarcoma cells [56] however the authors did not investigate if it was due to transfer of the TK mRNA, TK-protein or the toxic drug. It is also not known if GBM cells are also amenable to such mechanism. In this context, the mechanism of CD/5FC-associated BE has been studied in detail which has shown that the EVs play important role in CD/5FC BE. Altaenrova et al. reported that exosomes produced by CD-expressing mesenchymal stem cells (MSCs) contain the mRNA transcript of the suicide gene that can exert cytotoxicity in recipient cells [57]. It is not known if the mRNA or protein of TK can similarly be loaded into EVs. There is also a possibility that the toxic drug could be loaded into EVs and thereby mediate the BE in recipient cells, however the issue has not been investigated so far.

### 1.8 Extracellular vesicles and their role on intracellular signaling

In the last decades, the scientific interest describing the function of extracellular vesicles (EVs) and how they can be used in therapeutic applications hasexpanded substantially. Exosomes (Exos), microvesicles (MVs), apoptotic bodies (ApoBDs), microparticles, oncosomes and ectosomes are all different types of membrane structures released by cells that are commonly termed EVs [58]. These membrane-contained vesicles are released by both prokaryotes and eukaryotes. EVs are mediators of intercellular communication between cells due to their ability to carry several biomolecules and transfer proteins, lipids, nucleic acids and different types of RNA (mRNA, miRNA and other non-coding RNA), in an endocrine, paracrine and autocrine fashion [59]. Thus, EVs influence different physiological and pathological functions of both recipient and parental cells. Consequently, EVs are involved in many processes/diseases such as neuronal function, immune responses, neurogenerative diseases and cancer [60]. The content of the EVs and their biological functions depends on the cell of origin [61].

In 2014, The International Society for Extracellular Vesicles (ISEV) composed of researchers worldwide proposed guidelines with Minimal Information for Studies of Extracellular Vesicles (MISEV2014), which was again updated in 2018 (MISEV2018) [62].

### 1.8.1 Exosomes, Microvesicles and Apoptotic bodies

EVs, the general term for all secreted vesicles such as exosomes, microvesicles and apoptotic bodies, are found in body fluids such as urine and blood which makes them ideal carriers of biomarkers. Previously, they were considered as cellular trash due to their invisibility, small size, and lack of entity [59]. Exosomes are released upon fusion of multi-vesicular bodies (MVBs) with the plasma membrane, and are formed in the endosomal network in an inward budding process [58]. Exosomes are the smallest subtype among the EVs with a size ranging from 30-100 nm and cup-shaped in apperance under the electron microscope (EM) [60]. In contrast, microvesicles are formed in a process of outward budding and fission of the plasma membrane. MVs tend to be bigger in size ranging from 50 nm-1μm and are primarily distinguished from exosomes by its mode of biogenesis [63]. When cells undergo programmed cell death, apoptosis, the cytoskeleton breaks up and causes the membrane to bulge outward. Blebs of cells containing dying parts are released as apoptotic bodies in a multistep process in the extracellular space. This is a major mechanism among normal and cancerous cells. ApoBDs are generally larger in size compared to other EVs, ranging from 500-2000 nm [64]. After release, ApoBDs are removed via phagocytosis by macrophages *in vivo*. This is mediated by an interaction between the macrophages and surface proteins on the apoptotic membrane [63, 65].

Surface markers, method of isolation, size and the source of origin are the criteria that must be met to subclassify EVs into defined vesicles. However, circulating vesicles in fluids are prone to contain both exosomes and MVs, and unfortunately with purification methods available per today, it is still difficult to fully discriminate between them [66].

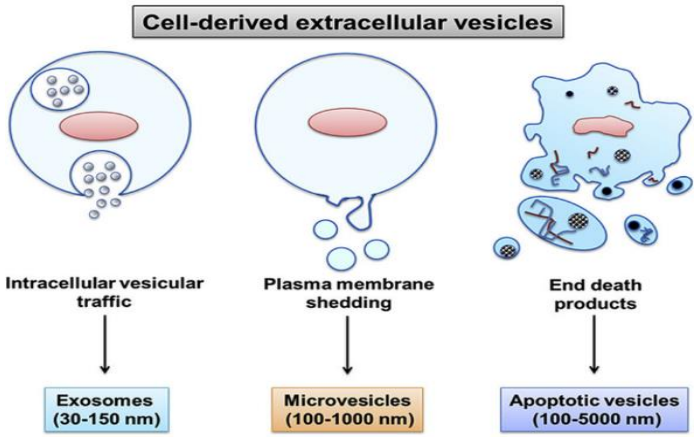


**Figure 1.7 Exosomes, Microvesicles and Apoptotic bodies.** Exosomes are released upon fusion of multi-vesicular bodies (MVBs) with the plasma membrane, while microvesicles are formed in a process of outward budding and fission of the plasma membrane. When cells apoptosis, the cytoskeleton breaks up and blebs of cells containing dying parts are released as apoptotic bodies. Figure adapted from [65]

### 1.8.2 Involvement of EVs in GBM

In the recent years research has clearly shown that GBM cells secrete EVs which are competent of escaping the tumor microenvironment and delivering genetic information to recipient cells that inflect their behavior[61] . GBM-secreted EVs have self-promoting features such as stimulating proliferation and angiogenesis in a pro-tumorigenic way. EVs secreted from tumor-cells can also engineer their surroundings in a benficial manner to tolerate tumor growth and invasion [67]. Skog et al., showed that GBM-secreted EVs from U87 glioma cells can stimulate proliferation of recipient cells. As demonstrated in additional studies, tumor-derived EVs support several hallmarks of cancer and better understanding of them will acknowledge novel diagnostic and therapeutic targets [61].

### 1.8.3 Methods for isolation of EVs

According to ISEV, a complete purification of EVs is not possible. There is no standardized single separation method and thus the choice of approach depends on the experimental question and final use of EVs [62]. Primary EV separation technique is ultracentrifugation-based, but alternative methods such as density gradients, immunoprecipitation, filtration and size exclusion chromatography and immunoisolation are also used [58]. Ultracentrifugation is the gold standard for

isolation today involving repeated centrifugation steps which results in larger and more dense particles sedimenting out first [30, 62].

### 1.8.4 EVs marker proteins

Isolated EVs are typically characterized by immunoblot analysis to demonstrate the presence of markers proteins or by transmission electron microscopy (TEM) to reveal a cup-shaped morphology [68]. Enrichment of these proteins in both exosomes and MVs is known to be highly dependent on the parental cell type [69]. Exosomes are enriched with endosome-associated proteins such as Annexins and flotilin due to their endocytic route. Other proteins such as Alix, TSG101, heat shock proteins, major histocompatibility complex (MHC) class I and MHC class II complexes and the tetraspanins CD9, CD81 and CD63 are often termed "exosomal markers" [70]. The abundance of tetrapanins and other proteins associated with the plasma membrane are commonly found in exosomes, and more enriched in these vesicles compared to cell lysates [70, 71]. Tetraspanins were suggested as specific markers for exosomes until studies revealed that these proteins could also be identified in MVs [72, 73]. MVs mainly contain cytosolic and plasma membrane associated proteins, such as tetraspanins. Proteins involved in post translational modifications, integrins, selectins and CD40 are all identified in MVs, however, the three latter are the main MV protein markers [66]. Nonetheless, specific markers that distinguish between MVs and exosomes have not yet been identified [70, 74]. In contrast to exosomes and MVs, ApoBDs contains small amounts of glycosylated proteins, chromatin and intact organelles. Annexin V, histones, and C3B and are used as molecular markers in larger EVs such as ApoBDs in some cell types [63, 75]. As suggested by ISEV, a set of marker proteins should be analyzed and either be enriched or absent from different EV populations [62].

# 2. Aims

The present thesis aims to explore the potential ability of extracellular vesicles such as exosomes, microvesicles and apoptotic bodies to increase the bystander effect of glioblastoma suicide gene therapy. . As explained in the introduction, the efficiency of SGT largely depends on the phenomenon called bystander effect (BE) whereby transduced cells transfer the already-metabolized toxic drug to the un-transduced tumor cells. As a result, the un-treated cells also undergo apoptosis. While gap junction-mediated BE is highly characterized in HSV-TK/GCV system, it is not properly clear if soluble factors such as apoptotic bodies, microvesicles and exosomes play any role in this process. In this project we are investigating the potential involvement of these soluble cellular factors in the process of HSV-TK/GCV-mediated BE. Our objectives are as follows:

- to analyze the HSV-TK/GCV-mediated cytotoxici effect on the secretion of extracellular vesicles
- to analyze the possible loading of HSV-TK.GFP protein in the extracellular vesicles and
  potential transfer thereof to other cells
- to analyze the cytotoxic effect following potential transfer of extracellular vesicles from TK-positive glioma cells

# 3. Materials and Methods

## 3.1 Cell culture

### 3.1.1 Media preparation

**Dulbecco's Modified Eagle's Medium (DMEM):** DMEM (Sigma-Aldrich Inc., St. Louis, MO, USA) was supplemented with 10% heat inactivated Fetal bovine serum (FBS) (Thermo Fischer Scientific, Waltham, MA, USA), 0.02% Plasmocin (Invitrogen, Toulouse, France), 2% (v/v) Penicillin-Streptomycin (BioWhittaker, Verviers, Belgium), 2% (v/v) L-glutamine (BioWhittaker), 3.2% non-essential amino acids (NEAA) (13-114E, Lonza, Walkersville MD USA). DMEM with all the supplements mentioned in this section is stated as complete DMEM throughout the thesis.

**Exosome Depleted Fetal Bovine Serum (FBS) Medium:**
Exosome depleted FBS was obtained by centrifuging (Beckman Coulter Optima LE-80 K ultracentrifuge) regular FBS in Quick-Seal Polypropylene centrifuge tubes (Beckman Coulter, Inc. 250 S, Kraemer Blvd. Brea, CA 92821, USA) for 18 hours at 40 000 rpm (179200 $g_{max}$) and 4°C using a Ti70 rotor (Type 70 Ti Fixed-Angle Titanium Rotor, Beckman Coulter, USA). Only the supernatant was retained and used. Further, the centrifuged exosome depleted FBS was filtered with 0.2 µm filter (Life Sciences, Acrodisc® Syringe filter) before 10 % was added to DMEM. The medium was alliquoted in 50 mL Falcon tubes and kept at – 20 °C.

**Exosome Depleted Fetal Bovine Serum (FBS) DMEM medium:** DMEM was supplemented with 10% exosome depleted FBS, 0.02% Plasmocin, 2% (v/v) Penicillin-Streptomycin, 2% (v/v) L-glutamine, and 3.2% NEAA. DMEM with all the supplements mentioned in this section is stated as exosome depleted DMEM throughout the thesis.

**Dulbecco's Modified Eagle's Medium (DMEM) with Ganciclovir (GCV):**
Complete DMEM supplemented with GCV (G2536, Sigma-Aldrich) to a final concentration of 25 µM.

**Exosome Depleted Fetal Bovine Serum (FBS) DMEM medium with GCV:**
Exosome depleted DMEM supplemented with GCV to a final concentration of 25 µM.

**Neurobasal Medium (NBM):** NBM was supplemented with 1% (v/v) Penicilin-Streptomycin, 1% (v/v) L-Glutamine, 2% (v/v) B27 Supplement (50X) ( Gibco™,Thermo Fisher Scientific, Waltham,MA,USA), , 0.1% Heparin LEO 5000 IE/ml (Vitusapotek), 20ng/ml Fibroblast Growth Factor-basic (bFGF) (100-18B, PeproTech®,Germany). It is stated as complete NBM throughout this thesis.

**Cell freezing media:** Complete DMEM was supplemented with 10% v/v Dimethyl sulfoxide (DMSO) (Sigma-Aldrich, Steinheim, Germany) and 10% v/v FBS.

### 3.1.2 Drug preparation

**Ganciclovir (GCV):**

**Table 3.1:** Information about GCV, modified from the Sigma Aldrich webpage [76]

| | |
|---|---|
| **Synonym:** | 9-(1,3-Dihydroxy-2-propoxymethyl) guanine;2¢-Nor-2¢-deoxyguanosine; 2¢-NDG; BIOLF-62; DHPG; BW-759U |
| **Application:** | GCV, a nucleoside analog that causes inhibition of viral DNA polymerase |
| **CAS Number:** | 82410-32-0 |
| **Molecular weight:** | 255.23 (Da) |
| **Molecular formula:** | $C_9H_{13}N_5O_4$ |
| **Appearance:** | Powder |
| **Physical state:** | Solid |
| **Solubility:** | Soluble at 10 mg/mL in 0.1. N HCl |
| **Storage:** | 2-8 °C |

Table 3.1 – displays important information about the prodrug used in this thesis, GCV (G2536, Sigma-Aldrich). The drug was received as powder and dissolved in complete DMEM to a final concentration of 3mM, aliquoted in 2.0 mL Eppendorf tubes (Eppendorf AG, Hamburg, Germany) and stored at -20 °C. New aliquot was used for each experiment, and stock solutions were thawed at room temperature (25 °C), and diluted in DMEM or exosome depleted DMEM to the required concentration.

### 3.1.3 Cell Lines

**U87:** U87, formally known as U-87 MG (Uppsala 87 Malignant Glioma) is a patient-derived primary GBM cell line, which was originally established at Uppsala University . This is a high grade glioma cell line that is commonly used in glioblastoma research. The cells are adherent and grows in monolayer. They exhibit epithelial morphology and were maintained in either complete or exosomes depleted DMEM until they reach the desired confluency.

**P3:** P3 is a patient-derived primary GBM cell line, which was established at Haukeland University Hospital, Bergen, Norway, generated from surgical resections. The cells are adherent and grows in monolayer, and they were maintained in complete NBM medium until they reached the desired confluency.

**U87.TK.GFP and P3.TK.GFP:** U87 cells were previously transduced with HSV-TK. 007 construct in the lab of Prof. Hrvoje Miletic. The lentiviral construct has previously been described in section 1.6.1 [77]. HSV.TK.007 transduced U87 and P3 cells were stated as U87.TK and P3.TK, respectively, throughout this thesis.

### 3.1.4 Sub-culturing and Passaging

Cell lines were kept in T175 culture flask (Nunc, Roskilde, Denmark) and maintained in a humidified incubator (Thermo Forma, Steri Cycle $CO_2$ Incubator, 301210-634, Ohio, USA) at 37 °C and 5% $CO_2$. Cell lines were subcultured at 75-80% confluency. Dulbecco's Phosphate buffer saline (PBS) (10X) (D1408, Sigma Aldrich, St Louis, Missouri, USA) diluted in autoclaved Milli-Q water (QGARD00R1, Millipore, France) to 1X working concentration was used as washing buffer. Nikon Eclipse TS100 (Nikon Corporation, Tokyo, Japan) inverted microscope was used to daily monitor the cells. All cell culture work was carried out in sterile condition under laminar flow bench (SANYO Electric Co, Osaka, Japan). The hood and equipment going in was sterilized with 70% ethanol before and after use.

**U87, U87.TK.GFP, P3, P3.TK.GFP:** Cell culture media was aspired, and the cell flasks were washed twice with 1x PBS. U87 cells were detached using Trypsin-EDTA (BioWhittaker) and incubated at 37 °C for 5 min. Trypsin process was neutralized with either complete DMEM or exosome depleted DMEM. P3 cells were deatched

from the buttom by scraping the surface with a cell scraper (VWR®, Pennsylvania, USA) and transferred to 15 ml tubes (Sarsted, Nümbrecht, Germany). The old media was removed by centrifugation at 300 g for 5 min, follwed by washing with 1x PBS. Both cell lines were resuspended in their respective media until single cell suspension was obtained. Resuspended cells were added to fresh flasks or counting. All cells were used for 15 passages post-thawing, one passage being considered as one trypsinization.

### 3.1.5 Cell counting

The cells were counted before *in vitro* experiments were performed. 100 µl of cell suspension was diluted in 400 µl Trypan blue dye (Life Technologies, OR, US) which is useful to differentiate dead and live cells based on the cell's ability to take up or exclude the dye. Live cells do not take up Trypan blue dye. 10 µl of diluted single cell/Trypan blue dye suspension was loaded to each chamber of hemocytometer (8100203, Neubauer, Hirschmann Laborgeräte GmbH & Co, Eberstadt, Germany) and covered with cover glass (Menzel-Gläser, Thermo Scientific). Hemocytometer consists of two identical chambers and each one has nine big squares of 1 $mm^2$ that are subdivided in three parallel lines with depth of 0.1 mm. Eight of the big squares have 16 squares whereas 1 big square in the center has 25 small squares. From each compartment, cells were counted from 4 big squares and the average was calculated. Cell concentration was calculated by following formula:

$$\textbf{Number of cells/ml} = \frac{\textbf{Total cell count x (Dilution Factor x } 10^4\textbf{)}}{\textbf{Number of squares counted}} * \textbf{5 trypan blue dillution factor}$$

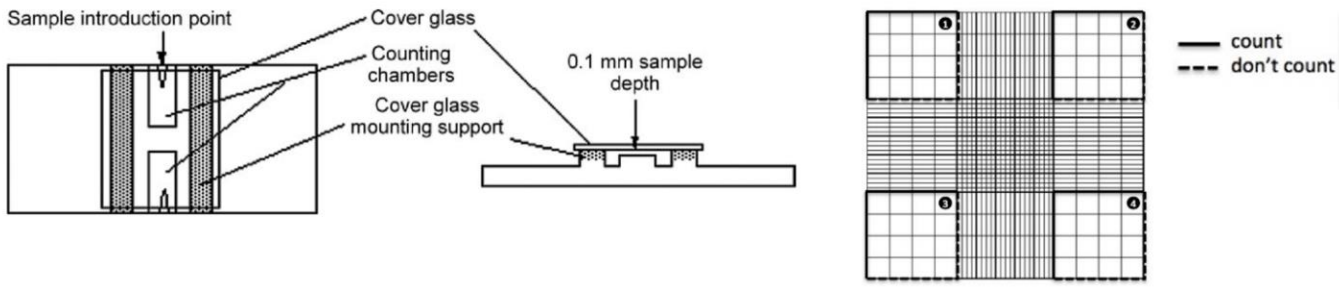


**Figure 3.1 Hematocytometer**. Left: Hematocytomter looked from the top. Right: Chamber of hematocytometer with 4 big squares. Cells presented on the dot lines were not counted. Figure adapted from [78].

### 3.1.6 Thawing and cryopreservation of cells

Cells were thawed by hand and immediately pipetted into a T75 $cm^2$ flask containing 15 mL of pre-warmed required media and resuspended gently prior to incubation at 37 °C, 5 % $CO_2$ and 100 % humidity. In order to remove remnants from freezing media, the cell culture media was replaced with fresh media after overnight incubation.

The cells were frozen down when a T175 $cm^2$ flask was 70-80 % confluent and after 10-20 passages in cryopreservation. After single cell suspension was obtain as described in section **3.1.3**, cells were transferred to a 15 mL Falcon tube (Thermo Scientific, NY, USA). The cell solution was centrifuged at 300 g for 5 minutes, the supernatant was removed, and the cell pellet was resuspended in cold freezing medium. 1.0 mL aliquots of cells were frozen in cryotubes (Nunc, Roskilde, Denmark) at -80°C in a Mr. Frosty™ Freezing Container (C1562, Sigma-Aldrich, Steinheim, Germany) overnight to provide a gradual temperature decrease. The next day, the cryotubes were transferred to liquid nitrogen tank for long time storage.

## 3.2 Isolation of EVs by ultracentrifugation

Prior to isolation of the EVs, the cell lines U87 and U87.TK.GFP were seeded in T175 $cm^2$ at a concentration of $15.0x10^6$ cells/35 mL in each flask. The cells were allowed to adhere for 24 hrs. before treating with condition media in the presence or absence of 25 µ M GCV. The day of isolation, the condition media was transferred directly from the flasks to 50 mL Falcon tubes. As negative controls, medium without drug for each cell line was used.

The ultracentrifugation is a multi-step process, where the falcon tubes containing media were initially placed in a low speed spin centrifuge (Eppendorf Centrifuge 5810 R (Sigma-Aldrich, Steinheim, Germany). In the first step, dead cells and other remnants were eliminated by centrifuging at 300 x g for 5 minutes. In order to collect apoptotic bodies, the supernatant from each falcon tube were transferred to clean tubes and spin down at 2000 x g for 20 minutes and 4 °C. Supernatant was transferred to quick seal centrifuge tubes through a syringe (50 mL, BD Luer-Lok syringe, Spain) to further harvest microvesicles, while pellet containing apoptotic bodies were put on ice. The centrifuge tubes were properly sealed using a sealing kit (Beckman Coulterm Cordless Tube Topper, Model: 7700, USA), placed in a fixed angle centrifuge rotor (Type 70 Ti Fixed-Angle Titanium Rotor, Beckman Coulter, USA) and further

installed in the Beckman Coulter ultracentrifuge. The samples were centrifuged for 22 minutes at 15 000 rpm (25200 $g_{max)}$ and 4 °C. Supernatant was removed from the tubes using a syringe and transferred to clean centrifuge tubes in order to collect exosomes from the cell condition media. The pellet containing microvesicles were put on ice. A final high-speed spin was performed at 40 000 rpm (179200 $g_{max}$ ) for 3 hrs. and 4 °C. The supernatant was discarded, and pellet containing exosomes saved on ice.

The different EVs pellet were resuspended in filtered 1X PBS, transferred to Eppendorf tubes, and stored at -80 °C for further characterization and analysis.

## 3.3 Western Immunoblotting

**Table 3.2- Reagents used for lysing the cells and EVs**

| Reagents Name | Composition |
|---|---|
| 1X PBS | 10 Phospho-buffered saline in MilliQ $H_2O$ |
| RIPA Buffer | Radradioimmunoassay precipitation buffer |
| Protease+Phophatase Inhibitors | 1 tablet protease inhibitors + 1 tablet phosphatase inhibitors in 1mL RIPA Buffer |

**Table 3.3- Reagents used for gel casting for SDS-PAGE.**

| Reagent | Composition (mL) | | |
|---|---|---|---|
| | Resolving, 12% | Stacking | Supplier |
| dH2O | 1.6 | 1.4 | |
| 30% acrylamide and bis-acrylamide solution | 2.0 | 0.33 | A3699, Sigma-Aldrich, UK |
| 1.5M Tris pH 8.8 | 1.3 | - | |
| 1.0M Tris pH 6.8 | - | 0.25 | |
| 10% Sodium Dodecyl Polyacrylamide (SDS) | 0.05 | 0.02 | |
| 10% Ammonium Persulfate (APS) | 0.05 | 0.02 | A3678, Sigma-Aldrich, St Louis, Missouri, USA |
| TEMED | 0.002 | 0.002 | T9281, Sigma-Aldrich, UK |

**Table 3.4- Reagents used for running, transfer and blotting of SDS-PAGE.**

| Reagents Name | Composition | Supplier |
|---|---|---|
| 1X SDS Tris-glycine | BioRad 10X TGS buffer in $dH_2O$ | 1610732, 10X Tris/Glycine/SDS Buffer, BioRad, USA |
| 1X Tris-Glycine transfer buffer | BioRad 10X TG buffer + 20% methanol in $dH_2O$ | |
| Ponceau stain | 0.1% Ponceau S in 5% Acetic Acid | P3504, Sigma-Aldrich, St. Louis, Missouri USA |
| 5% blocking buffer | 5% Skim milk powder in TBS-Tween Buffer | |
| TBS-Tween Buffer | 0.02 M Tris-HCl (pH 7.5), 0.15 M NaCl and 0.1% Tween 20 | |
| 1X TBS | Tris-Buffered Saline (0.2 M Tris-HCl (pH 7.5), 1.5 M NaCl) in $dH_2O$ | |

To characterize and confirm successful harvest, the EVs from U87 and U87.TK +GCV/control were subjected to western immunoblotting. Cell lysates s were also included. After condition media was removed in order to collect the EVs, the adherent cells were washed with cold PBS, trypsiniezed, and counted in order to indicate % dead cells at the time of harvest. Following, transferred to 15 mL tubes and centrifuged at 3000 rpm for 5 minutes at 4˚C.

### 3.3.1 Protein concentration determination

The cell pellet and isolated EVs were lysed by using Radioimmunoassay precipitation buffer, RIPA, supplemented with 10% protease (04693124001, Roche, Manheim, Germany) and phosphatase (04906845001, Roche, Indianapolis, USA) inhibitors. The protein concentration in each EV and lysate was determined using Pierce™ BCA Protein Assay Kit (Pierce Biotechnology, Rockford, lL, USA). With the relative absorbance measured with Direct Detect® Spectrometer (DDHW00010-WW, Merck Millipore, USA), we could make a calibration curve to determine the concentration of each sample.

### 3.3.2 Gel Casting, Sample Preparation, SDS-PAGE, antibody incubation and protein detection

12% Tris-Glycine Sodium Dodecyl Sulfate (SDS)-polyacrylamide gels were freshly casted before each western blot accordance to table __ in use of Mini-PROTEAN® Tetra Hand Cast System (Bio-Rad, Hercules, California, USA). Samples were thawed

on ice with 25 µg total protein of each sample mixed with 5x Loading buffer (along with reducing agent and beta mercaptoethanol) and Milli-Q water was added until the desired volume was reached. The cell lysate mixture and the EVs mixture were then heated for 10 minutes at 70˚C and 5 minutes at 95 ˚C respectively and spin down before loading on the gel. Precision Plus Protein Western C Standards (L001652A, USA) was used as protein marker size and loaded onto the first well of the gel. Equal amount of each samples were added to the remaining wells. Gels were run at 80 V (Bio-Rad Electrophoresis Power Supplier) for 30 min for protein stacking, and then at 100 V for protein separation, in an electrophoresis chamber (BioRad, USA) filled with premade Tris-glycine running buffer. SDS-PAGE is a technique that allows separation of proteins based on their molecular weight. SDS is an anionic detergent used to denature proteins and it provides with an overall negative charge. In application of electric field, the smallest proteins migrate faster than the larger ones towards positive pole.

Proteins separated on gel were transferred onto 0.2 µM pore nitrocellulose membranes (Bio-Rad laboratories AB, Oslo, Norway) by using the BioRad Mini Trans-Blot® transfer system. Blotting sponges, filter papers and the membrane were soaked in chilled Tris-Glycine transfer buffer and assembled (Figure 3.2) a small rolling pin was used to remove the air bubbles between the layers. Chamber filled with transfer buffer was placed on ice and the electrophoresis was run at 45 V for 90 min in use of Invitrogen PowerEase 300W.

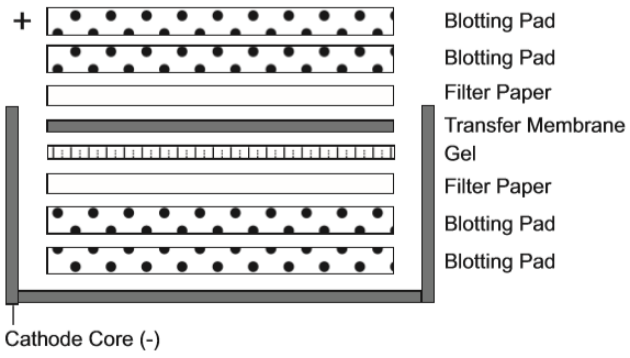


**Figure 3.2 Immunoblot sandwich.** Correct way to asseble the sandwich, where the gel is allowed to be attached with the nitrocellulose membrane in order to have successful transfer of the proteins. Figure is adapted from NuPAGE® Technical Guide [79].

The membrane was stained with Ponceau S for 2 mins to visualize total proteins band and to confirm successful transfer. Following, the membrane was cut according to the molecular weight of the proteins of interest and subjected to blocking in 5% skim milk buffer for 1 hour at room temperature. This step is important to prevent unspecific binding of antibodies to other bindings sites on the membrane. Primary incubation of membranes were performed overnight at 4°C on a shaker with corresponding primary antibodies diluted in 5% skim milk TBS-T (Table 3.5). Membranes were washed 3 x 10 mins in TBS-Tween washing Buffer before adding Horseradish Peroxidase (HRP) conjugated secondary antibody of the host species of primary antibody for 1 hour at room temperature on a shaker. All the secondary antibodies (Table 3.5) were diluted in blocking buffer.

**Table 3.5 Primary and Secondary Antibodies used for immunoblotting**

| **Primary Antibody** | **Supplier** | **Catalogue Number** | **MW (kDa)** | **Dilution** | **Host** | **Buffer** |
|---|---|---|---|---|---|---|
| Calnexin | Santa Cruz Biotech. | 46669 | ~ 90 | 1:1000 | Mouse | 5% skim milk TBS-T |
| CD81 | Santa Cruz Biotech. | 166028 | ~ 22-26 | 1:200 | Mouse | 5% skim milk TBS-T |
| GFP | EMD Millipore | AB3080 | ~ 70 | 1:6000 | Rabbit | 5% skim milk TBS-T |
| **Secondary Antibody** | | **Supplier** | **Catalogue Number** | **Dilution** | **Buffer** | |
| Goat anti-Mouse IgG (H+L), HRP | | Invitrogen USA | 31430 | 1:10000 | 5% skim milk TBS-T | |
| Goat anti-Rabbit IgG (H+L), HRP | | Invitrogen USA | 31462 | 1:10000 | 5% skim milk TBS-T | |

Prior to detection of proteins, the membranes were washed 3 x 10 mins to get rid of unbound secondary antibodies. The visualizing was performed using Image Reader LAS-3000 (Fujifilm Medical System Inc., Connecticut, USA) and chemiluminescent detection kit, either SuperSignal™ West Pico PLUS Chemiluminescent Substrate or/and SuperSignal™ West Femto Maximum Sensitivity Substrate (34080, 34096, Thermo Fisher Scientific, Waltham, USA. the membranes were developed in increment mode at intervals of 10 seconds. Images were analyzed using a combination of Multi Gauge software and Image J (USA).

### 3.4 Statistical Analysis

All statistical analyses were performed using GraphPad Prism8.2.1 The realtive band intensity significance from immunublotting was analysed by one sample t test and Wilcoxon test. P-values less than 0.05 were considered as significant.

**One sample t-test and Wilcoxon test:** $^{ns}P>0.05$, $^{*}P<0.05$,

### 3.5 Transmission electron microscopy (TEM)

TEM was performed to confirm the presence of different EVs and to analyze the morphology and size. This technique allows to characterize very small objects/particles with 1µm to 1 nm in size. TEM consists of an electron emission source, electromagnetic lenses and an electron detector. It is based on a beam of highly energetic electrons released by an electron gun that pass through a sample within a high vacuum. When the beam passes through, the electrons are absorbed differently by different areas of a sample. The sample modifies the beam and imprint its conventional image. The electrons are captured from below the sample onto a phosphorescent screen or through a camera[80]

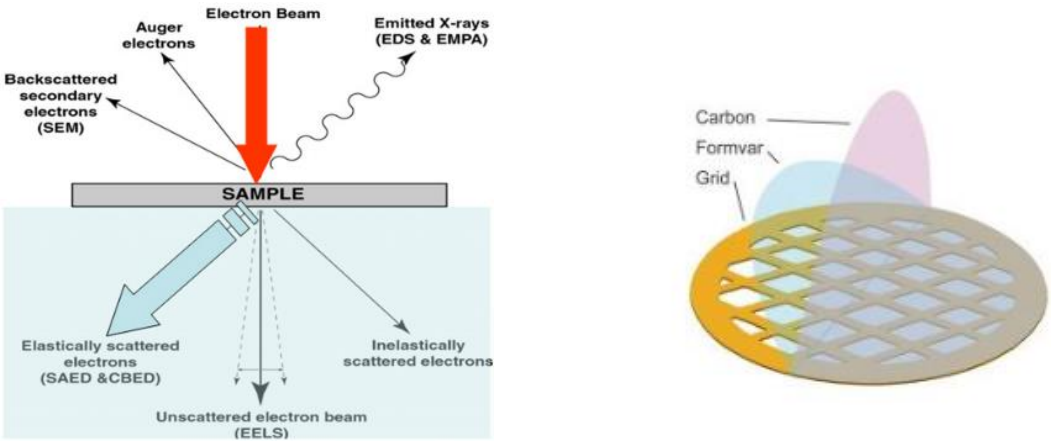


**Figure 3.3 Transmission Electron Microscopy (TEM) overview.** Left: Electron beam pasing through a sample and scattered by the sample. Figure adapted from [80] Right: Crabon coated copper grid used to mount samples on. Figure adapted from [81]

10 µg of EVs protein of the intact EVs resuspended in PBS was dropwise placed on a parafilm. With forceps, a formvar carbon coated copper grid with 200 mesh was positioned with the coating side facing the drop containing EVs of interest for 15 mins. 3 drops of PBS was placed on the parafilm, and the grid was washed

sequentially on top of each droplets. Absorbing paper was used between every washing step. Following, 2,5% glutaraldehyde (25% glutaraldehyde stock solution diluted in 0.1 M sodium cacodylate) was placed on the parafilm to post-fix the samples. Following 10 mins incubation, the grid was subjected to 5 droplets of deionized water for washing. The sample was contrasted by adding the grid on a droplet of 2% uranyl acetate and incubating for 10 mins. Excess liquid was removed and grid with the coated side facing up was dried for 5 mins. The prepared grid was either examined by TEM or stored in a grid box for later examination.

The grid was examined with Jeol Jem-1230 transmission electron microscope at 80 kV, and images captured with MultiScan Camera (Gatan) model 791.

### 3.6 Mass spectrometry (MS)

We performed mass spectrometry to check the protein composition in the EVs, commonly EV- associated proteins and to show if the abundance/expression of these proteins is different in treated vs. untreated vesicles. The principle behind MS and how the data is interpreted in the MaxQuant proteomic software is to be found in Appendix I.

### 3.7 Vesicle Transfer Assay

#### 3.7.1 Labeling of exosomes with PKH67

The PKH67 Green Fluorescent Cell Linker Kit (Sigma-Aldrich, USA) consisting of diluent C and PKH67 dye was prepared in such a way ending up with $4 \times 10^{-6}$ M PKH67 dye. The samples were prepared by taking out 25 µL (equivalent to 25 µg) of exosomes resuspended in PBS and 25 µl PBS which act as control without exosomes. Diluent C was added to exosomes and control to a total volume of 1 mL. Following, the exosomes/diluent C mixture was added to dye/diluent C mixture and incubated for 5 minutes with periodically intermittent pipetting. 1% BSA was added to the samples and control in order to prevent unwanted binding of the dye. Later, the PKH67 stained exosomes and ctrl were transferred to PBS pre-wet 300kDa filter (Vivaspin filters). Filters containing the samples were centrifuged at 4000 x g in short periods to make sure a small part of the sample was remaining on the top. Samples were then washed

twice with PBS at 4000 x g and transferred to new pre-wet 300 kDa filters. Exo dep. DMEM was added and a last centrifugation step was performed to complete the staining of the exosomes.

24 hrs. prior to exosome staining, 5.0 x $10^4$ cells were seeded in a 6-well plate. A coverslip was placed in every well, and the cell suspension was carefully added so the cells were allowed to adhere on the surface of the coverslip for 24 hrs. The stained exosomes and control was added to respective wells and incubated at 37 ° C for 24 and 48 hrs.

### 3.7.2 Cell fixation with Paraformaldehyde (PFA)

Before visualizing the uptake kinetics with microscope, the cells were fixed 24 and 48 hrs. post exosome incubation. The old media from the 6-well plate was aspirated and washed with PBS twice. Following, the cells were incubated with 4 % PFA for 15 mins at room temperature to allow fixation. Then washed with PBS and subsequent with water to rinse of PBS in order to avoid formation of crystals. The coverslips were gently placed on a slide containing a droplet of Vetashiled mounting medium. The slides were allowed to dry overnight at RT.

### 3.7.3 Confocal microscopy

The uptake of the exosomes into the GBM cells was visualized by Leica TCS SP8 STED (stimulation emission depleted) 3X confocal microcopy. In principal, confocal microscope uses fluorescence optics, where the laser light focused onto a define spot resulting in emission of fluorescent light only from that particular area. A light detector will only sense fluorescence signal from the illuminated spot, while a pinhole blocks any other scattered light emitting from the sample. Raster scanning pattern of a specimen creates images with one single optical plane [82].
Leica TCS SP8 STED provides with super-resolution that allows to visualize structure smaller than ~ 200 nm. It matches the wavelength of any fluorophore and allows for up to eight excitation lines usage simultaneously with its white light laser source. But, the peak excitation wavelength and the emission wavelength of two different proteins must be separated by 50-60 nm in order to be sensed by two distinct fluorescent channels. The emitted fluorescence light is sensed by a Hybrid-gated detector [83].

### 3.8 WST-1 Cytotoxicity Assay

We wanted to investigate if TK. mRNA or protein and GCVp, GCVpp or GCVppp could induce any potential cytotoxicity onto naïve U87 by traveling through EVs. We approach this by performing WST-1 assay which is a technique used to measure cell proliferation and viability. Water soluble tetrazolium (WST) salts are produced by adding positive or negative charges and hydroxy groups to phenyl ring of the tetrazolium salt. WST-1 (Cell Proliferation Reagent WST-1, 11644807001, Roche, Mannheim, Germany) is not able to pass through the cell membrane due to its negative charge. Mitochondrial dehydrogenase acts as an intermediate electron acceptor and transfer electrons from the plasma membrane to cytoplasm for the reduction of tetrazolium into a soluble formazan dye. Only the viable cells are able to reduce tetrazolium to formazan, so the amount of formazan produced correlates with the metabolically active cells.

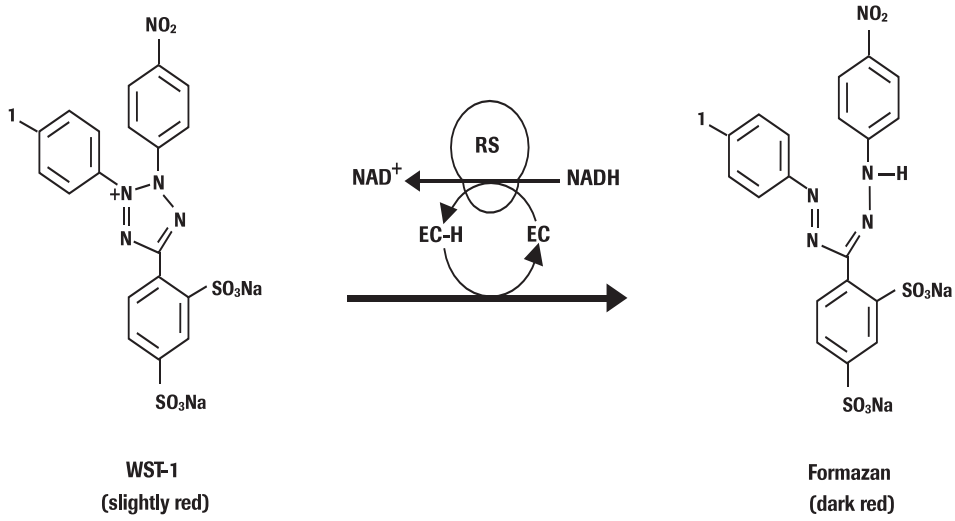


**Figure 3.6 Tetrazolium salt WST-1 cleaved to formazan.** Cellular enzymes cleave the tetrazolium salt into formazan, and the amount of formazan dye produced correlates with the number of viable cells in the culture. Figure is adapted from Cell proliferation Reagent WST-1 datasheet [84].

U87 cells were washed, trypsinized and seeded in 96-well plates in a density of 1.5 x $10^4$ cells/100 µL exo dep. DMEM in 5 replicates. The set up for potential cytotoxicity by TK. mRNA or the protein is shown in table3.6. 8 hrs. post-seeding, a final GCV concentration of 25 µM was added to the specific wells. After 96 hrs., an el-pipette was used to achieve precise addition of 7µL WST in each well and incubated for 1 hr., before scanning the plate by spectrophotometer.

**Table- 3.6. Overview of sample preparation for cytotoxicity assay**

| Sample nr. | Sample | EV from | GCV | Potential cytotoxcity |
|---|---|---|---|---|
| 1 | U87 | - | - | - |
| 2 | U87 | - | 25 µM | - |
| 3 | U87 | U87.TK | - | - |
| 4 | U87 | U87.TK | 25 µM | Yes/No |

# 4. Results

## 4.1 Analysis of EV secretion in glioma cells

U87, a widely used human glioma cell line [85] is known to secrete EVs [67] . First, we needed to confirm EV secretion in our model system where we used U87 cells that previously have been modified by lentiviral vectors in our laboratory to express TK-GFP (hereafter designated as U87.TK). To investigate the secretion and confirm successful harvest of EVs, U87 and U87.TK cells were grown as adherent monolayers cultured in exosome depleted culture medium as described in the methods section. Isolated EVs were subjected to immunoblotting by using antibodies against the tetrapanins CD9, CD63 and CD81 which serve as markers for both exosomes and MVs. Enrichment of these proteins in both exosomes and MVs is known to be highly dependent on the parental cell type [69]. CD81 showed the most consistent enrichment in exosomes and MVs and was therefore selected to be further used for the detection of exosomes and MVs in this project (figure 4.1). Calnexin, an integral protein derived from the endoplasmatic reticulum (ER), was used as a negative control for MVs and exosomes, but was found to be present in the ApoBDs. ApoBDs are known to be larger vesicles than the two other EVs subtypes based on size and more likely to incorporate a larger amount of RNA/protein or organelles. The absence of calnexin in other lanes indicate that MVs and exosomes did not contain ER contaminants.

To further confirm the enrichment of CD81 in the exosomes and MVs we used P3 cells which are human stem-like glioma cells cultured in serum-free neurobasal medium. We observed enrichment of CD81 in exosomes and MVs harvested from P3 and TK-modified P3 cells (designated as P3.TK) (Figure 4.2). Thus, the secretion and successful harvest of the exosomes and MVs was confirmed in two different glioma cell lines.

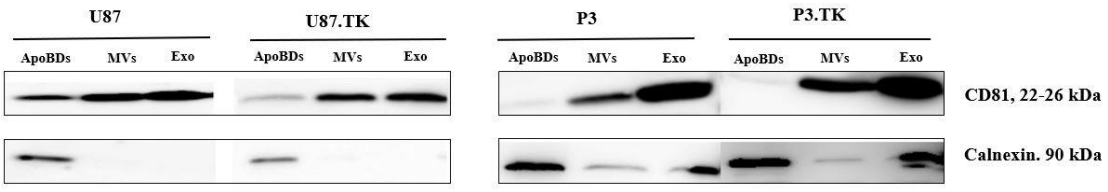


**Figure 4.1 Characterization of EVs from U87/U87.TK and P3/P3.TK cells by immunoblotting.** The presence of EVs in two different glioma cell lines, U87/U87.TK and P3/P3.TK were confirmed by immunoblotting. CD81, an exosomal enrichment marker was found to be present in exosomes and MVs confirming successful secretion of these EVs. The blot is representation of 3 individual experiments. ApoBDs – Apoptotic Bodies, MVs – Microvesicles, Exo –Exosomes.

While immunoblotting confirmed successful secretion of EVs in our model system, we further performed microscopic analyses using Transmission electron microscopy (TEM) to validate these observations. Figure 4.2 A, B and C shows the images obtained from EVs secreted from U87 and U87.TK. The EVs were abundant and appeared to be of typical cup-shaped structure. ApoBDs are known to have size that ranges between 500 nm to 5000 nm [86]. In our experimental setting, we observed larger vesicles in GCV treated U87.TK cells corresponding to ApoBDs, however, we found smaller vesicles of size similar to exosomes and MVs in U87 WT and U87 TK ApoBDs fractions. This suggests that the pelleting of ApoBDs at 2000 x *g* centrifugal speed is also pelleting exosomes-like vesicles along with ApoBDs, indicating exosomal contaminants in ApoBDs fractions. In all isolates from the three different cell types, MVs and exosomes showed cup-shaped lipid bilayer membrane structures and sizes similar to the ones previously reported by other research groups [87] [86]. This demonstrates that the presence of EVs in the culture media of U87 and U87.TK cells and their successful harvest were confirmed by both immunoblotting and TEM.

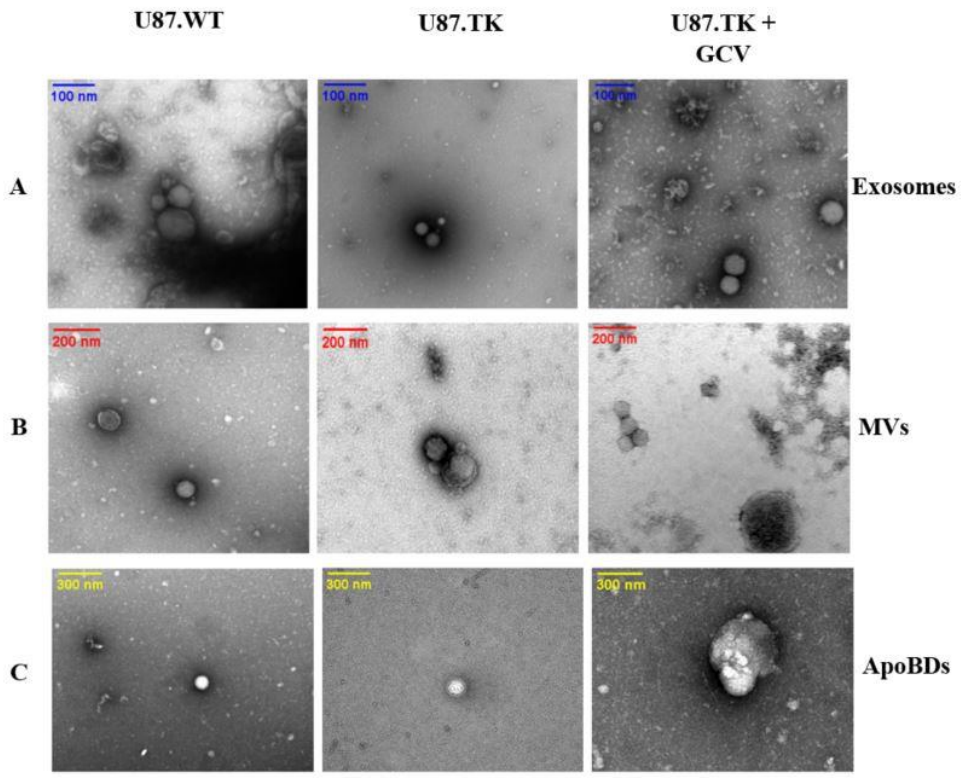


**4.2. Analysis of EVs from GBM cells by Transmission electron microscopy.** Micrographs of vesicles, negatively stained, released from three different cell lines; U87 WT, U87.TK and U87.TK+GCV are shown. A-panel shows exosomes vesicles that are cup shaped and have diameter between 40-120nm. B-panel displayed MVs that have sizes between 100nm to 250nm and were diverse in shape and density. C-panel displayed fractions of ApoBDs that were pelleted at 2000 x *g* showed exosomes like vesicles that were pelleted with ApoBDs with a size ranges between 80-400nm in our experiments. Scale bar: Exosomes – 100nm, MVs – 200nm and ApoBDs – 300nm. (n=3) ApoBDs – Apoptotic Bodies, MVs – Microvesicles, Exo –Exosomes.

### 4.2. The Effect of GCV-mediated cell death on the secretion of exosomes and MVs in GBM cells

To unravel the involvement of ApoBDs, MVs and exosomes in the bystander effect during TK/GCV therapy in GBM cells, it is important to identify the effect of GCV-mediated cell death on the secretion of EVs. First, we performed mass spectrometry with extensive analysis of the proteome where we identified more than 1500 different proteins in all samples (Table 4.1). Based on a heat map with supervised clustering (see Appendix II, figure 4.10) we identified two large separate clusters, with cell lysates in one group, whereas EVs clustered together in a separate group. We also identified a modest increase of proteins in samples treated with GCV (see Appendix II, Figure 4.11).

**Table 4.1- Total identified proteins**

| Sample Type | Total identified proteins |
|---|---|
| TK Exosomes | 1662 |
| TK Exosomes + GCV | 1925 |
| TK MVs | 1528 |
| TK MVs + GCV | 1713 |
| TK ApoBDs | 2248 |
| TK ApoBDs + GCV | 2544 |
| TK Cell lysate | 1963 |
| TK Cell lysate + GCV | 2326 |

Next, we wanted to identify if there were any differences in enrichment of proteins that are normally presented in EVs such as CD9, CD81 and TSG101. In the heatmap (Figure 4.3), the different types of EVs clustered together which was independent of the treatment. However, we also identified differences in the expression of specific proteins following GCV treatment. We observed upregulation of CD9 and CD81 in GCV-treated exosomes and MVs, while a downregulation of the same proteins was found in GCV-treated ApoBDs (Figure 4.4). Determination of relative intensity further demonstrated that CD9 and CD81 are more abundant in GCV-treated exosomes and MVs, but not in cell lysates indicating that GCV-mediated cell death increases secretion of exosomes and MVs.

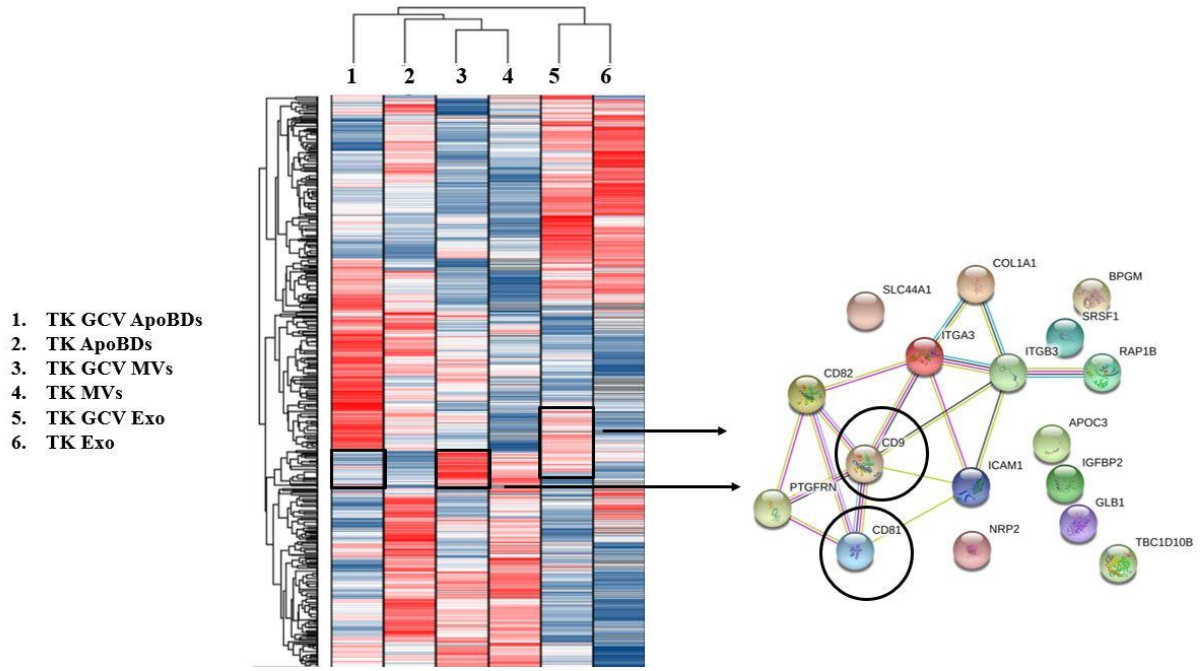


**Figure 4.3 Upregulation of key marker proteins of exosomes and MVs:.** Mass spectrometry analysis revealed that CD81 and CD9 is upregulated in treated exosomes and MVs, while it is downregulated in treated ApoBDs

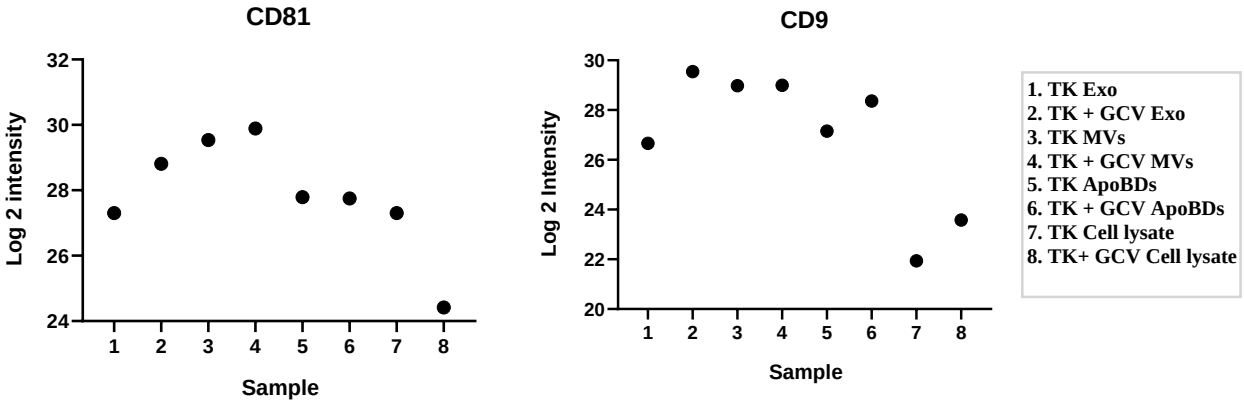


**Figure 4.4 Increased CD81 and CD9 in EVs following GCV treatment.** Increase of CD9 and CD81 in treated exosomes is clearly observed. The difference in MVs and ApoBDs is modest. Included are imputed values from mass spectrometry

Originally, we planned to further analyze the harvested vesicles by using a particle counter (Zeta View Nanoparticle Tracking Analysis, NTA) to assess and quantify the amount of secreted EVs with our collaborator at the University of Gothenburg. Unfortunately, due to the unexpected events created by the coronavirus outbreak we were not able to perform this experiment. Instead, we decided to use semi-quantitative immunoblotting with anti-CD81 antibodies on lysates from exosomes and MVs from TK. GFP + GCV cells and TK.GFP cells from three independent experiments. (Figure 4.5 A). CD81 was also detected in ApoBDs fractions, however mostly at a lower level compared to other EV subtypes. Interestingly, we observed a trend of increased expression of CD81 in EVs from cells treated with GCV versus untreated (UT) cells, however the difference was not significant for exosomes and ApoBDs, but for MVs. Importantly, this trend was not found in the cell lysates.

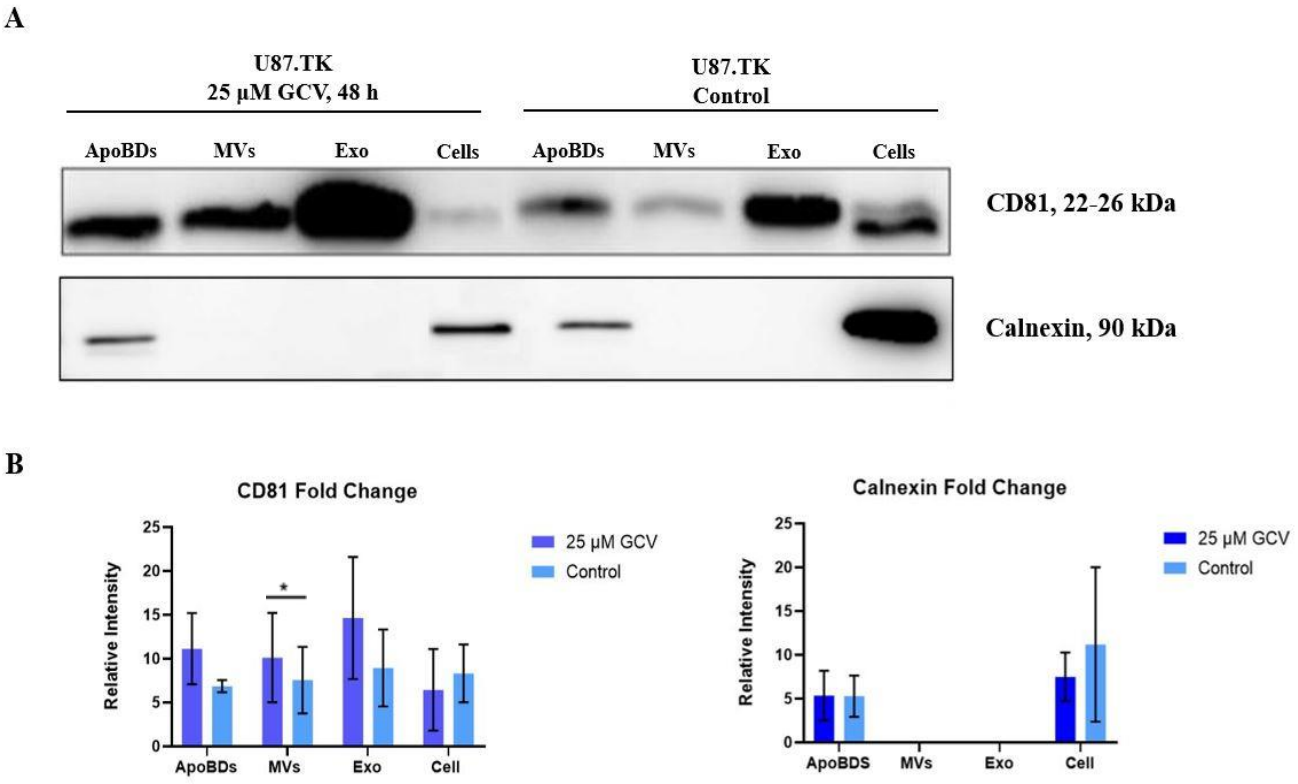


**Figure 4.5 Analysis of extent of EVs secretion by using immunoblotting .** A. One representative (out of 3) experiment. Increased CD81 is detected in the EVs following GCV-treatment. Calnexin is included as a negative control for exosomes and MVs . Cell lysates are included as control samples. **B.** Statistical analysis was performed by using One sample t test and Wilcoxon test. The significant increase of CD81 was only confirmed between untreated MVs and GCV-treated MVs. $P<0.05$. ApoBDs – Apoptotic Bodies, MVs – Microvesicles, Exo – Exosomes.

### 4.3 TK.GFP protein is loaded in the EVs of GBM cells

As we have shown in the previous sections that EVs are secreted during suicide gene therapy, we aimed to investigate whether the secreted EVs contained the TK.GFP protein which could potentially contribute to the BE during HSV-TK/GCV therapy. GFP is a fusion protein that is not expressed independently from TK. We used both immunoblotting and mass spectrometry to detect the presence of TK.

EVs harvested from U87.TK cells (with or without GCV treatment) and U87.WT cells were analyzed by immunoblotting with anti-GFP and anti-CD81 antibodies. The molecular weight of HSV.TK is around 40 kDa, but as it is fused to GFP with approximately 27 kDa, we anticipated bands at around 70 kDa. GFP is a fusion protein that is not expressed independently of TK. As expected, (Figure 4.6), bands were observed in the cellular fraction of U87.TK cells but not in U87. CD81 expression confirmed the presence of exosome and MVs in these fractions. Our result indicates that the TK.GFP fusion protein is loaded in the EVs. To further confirm this result, we performed mass spectrometry analysis.

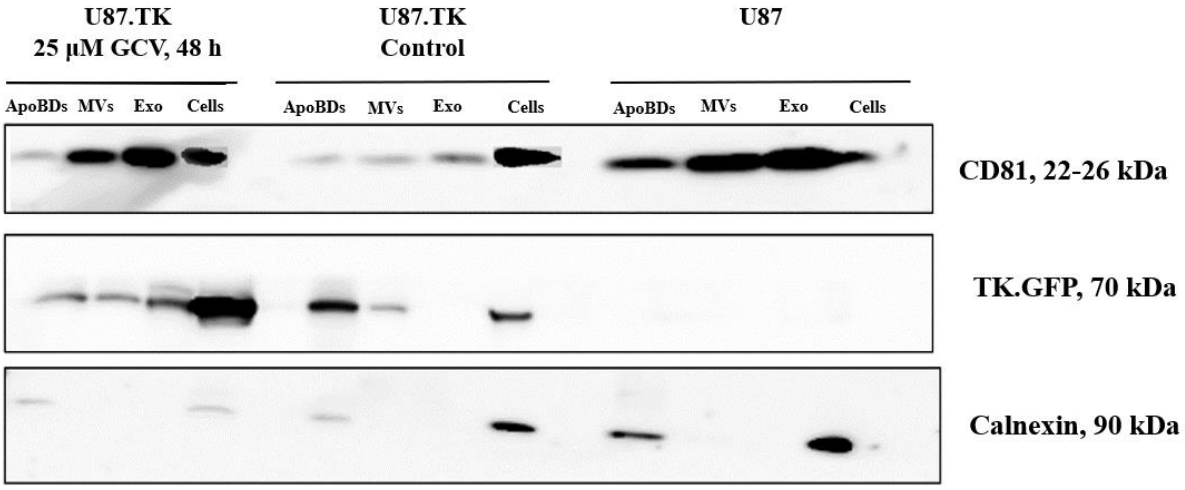


**Figure 4.6 Confirmation of TK.GFP in the vesicles by immunoblotting.** The presence of exosomes, MVs, ApoBDs and cell lysate in U87, U87. TK and U87.TK +GCV is confimed with CD81 and Calnexin. Our result indicates that the TK-GFP fusion protein is loaded in the EVs, but the expression in U87.TK exosomes are low.

Our mass spectrometry data revealed that the HSV-TK and GFP protein is present in all fractions secreted from U87.TK cells (Figure 4.7). There was no clear expression of the TK.GFP in wild-type U87 cells and their EV subtypes as expected. Interestingly, the enrichment of GFP and HSV.TK increases in MVs and ApoBDs from GCV treated TK cells, compared to the untreated TK cells. There were no significant changes observed between exosomes from both the cell types. The GCV-treated ApoBDs showed the highest expression of TK. Thus, we demonstrated that the TK-protein is loaded into the EVs.

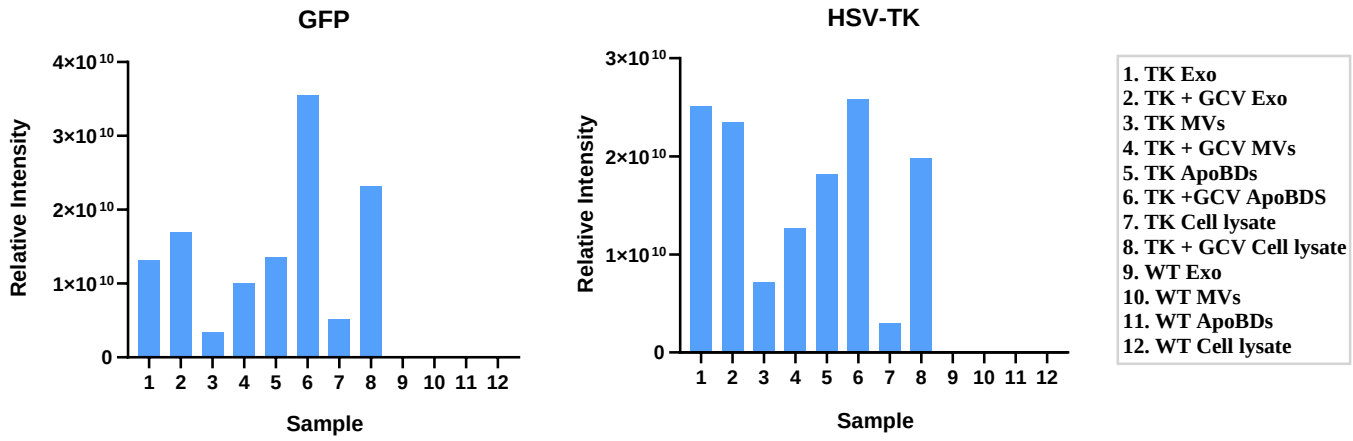


**Figure 4.7 Confirmation of HSV.TK and GFP protein in the vesicles by mass spectrometry**
The presence of exosomes, MVs, ApoBDs and cell lysate in U87, U87. TK and U87.TK +GCV is confirmed with CD81 and Calnexin. Our results indicate that the TK-GFP fusion protein is loaded into the EVs.

### 4.4 Transfer of EVs to other cells

After confirming that EVs contain the TK-GFP protein as cargo it would be important to analyze whether the EVs are capable of transferring the suicide gene product into recipient cells. To study this transfer, we planned to exploit PKH26 dyes that would stain the EVs and would discriminate from the cells stained with blue nuclear dye and green cytoplasm due to the GFP-tagged TK protein. However, to optimize the protocol, we first performed a pilot experiment to analyze if the exosomes are being transferred at all. In this pilot experiment, we labelled exosomes with PKH67 green dye (ex: 490 nm and em: 502 nm) and the nucleus of the cells with DAPI staining. When imaging with confocal microscopy we observed that the blue nucleus of the U87 recipient cells were surrounded by small green dots (Figure 4.8). The negative control is a PBS/medium control that was included to show the unbound form of dye without vesicles that was washed out during filtration. Our results suggest that the exosomes are likely transferred to recipient cells, however, we could not verify if the exosomes are inside the recipient cells or just attached to the outer cell membrane.

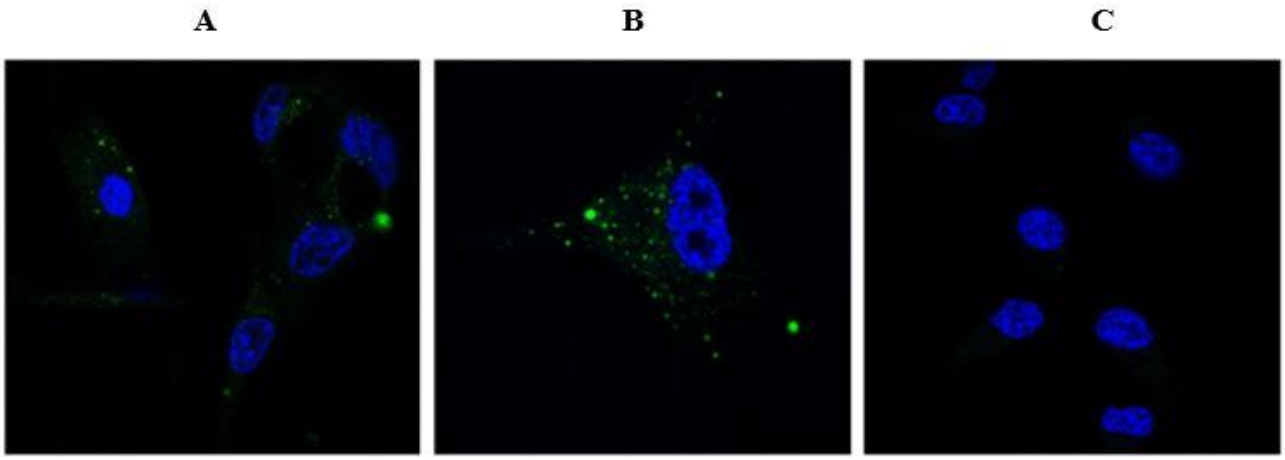


**Figure 4.8 Exosome transfer assay visualized with confocal microscopy.** Panel A & B: Dapi stained nucleus surrounded by exosomes stained in green, Panel C: Negative control, shows only cells.

### 4.5 Cytotoxic effect of ApoBDs from TK-positive glioma cells

As our results indicated that TK could be transferred through secreted vesicles from donor to recipient TK-negative cells, we wanted to investigate if the transferred protein could induce a potential cytotoxicity on naïve U87 by traveling through EVs. The mass spectrometry results (section 4.3) revealed that the abundance of TK protein was highest in ApoBDs and therefore we chose to first proceed with this vesicle subtype.

96 hrs post incubation of U87.TK-derived ApoBDs with U87 naïve cells revealed the presence of the ApoBDs in the culture medium and the fluorescence emitted green light confirmed the presence of TK-GFP protein in the ApoBDs (Figure 4.9).

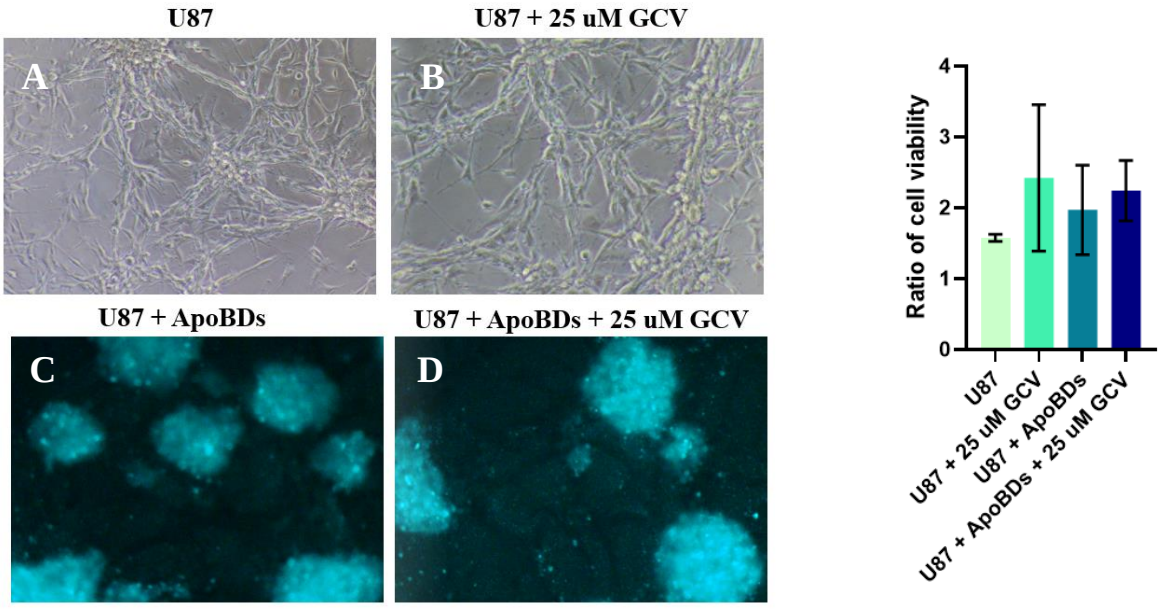


**Figure 4.9 Cytotoxicity assay with ApoBDs.** Left: A. Only U87 naïve cells. B) U87 naïve cells treated with GCV after 8 hrs. C) U87 naïve cells treated with ApoBDs loaded with TK protein. D) U87 naïve cells treated with ApoBDs containing TK protein and GCV. Right: Ratio of cell viability. Do not observe increased suicide activity in U87 cells treated with ApoBDs and GCV. Represent only one experiment.

After verifying the presence of TK.GFP in the ApoBDs we performed a cytotoxicity assay to analyze potential contribution of ApoBDs to the BE through uptake into naïve cells. However, we could not identify any significant differences in cell cytotoxicity between control or cells treated with ApoBDs and/or GCV (Figure 4.9).

# 5.Discussion

The highly aggressive and invasive nature of GBM limits the outcome of standard therapy which involves safe surgical resection, followed by radiotherapy (RT) and concomitant chemotherapy with TMZ [30]. This resistance to conventional treatments, which in addition is caused by tumor heterogeneity and a highly immunosuppressive microenvironment results in poor survival outcome and high mortality rate [31].

Suicide gene therapy is a promising treatment alternative which converts a nontoxic prodrug into a cytotoxic drug that kills dividing tumor cells. It has been shown in earlier studies that the metabolized cytotoxic drug spreads to neighboring cells through gap junctions to execute BE [53, 54]. While gap junction-mediated BE is highly characterized in the HSV-TK/GCV system, it is not properly clear if soluble factors such as ApoBDs, MVs and exosomes play any role in this process. In addition to the BE mediated by the toxic drug, it is, in theory possible, that mRNA or protein of the suicide gene could be transferred from the TK-transduced cells via EVs during HSV-TK/GCV suicide gene therapy. In this regard, the involvement of EVs in the mechanism of BE has been studied in CD/5FC mediated SGT, which is another widely used SGT system. It has been reported that exosomes produced by CD-expressing MSCs contain the mRNA transcript of the suicide gene which can cause cytotoxicity in neighboring cells [57]. In the TK/GCV system, the involvement of ApoBD-mediated BE has been suggested, but not conclusively determined [56]. Furthermore, it was not investigated if the ApoBD-mediated BE was caused by the transfer of TK mRNA, TK-protein, or the toxic drug [56] . In addition, the involvement of exosomes and MVs has not been investigated in the context of TK/GCV-mediated SGT. The objective of this thesis was to analyze the potential involvement (and mechanism) of EVs in BE of HSV-TK/GCV therapy.

Hypothetically, an EV-mediated BE can be executed through 3 major routes: 1) transfer of TK mRNA that can be translated into active protein in the recipient cells, 2) transfer of TK protein and 3) transfer of phosphorylated GCV. In this project, our major focus was on the potential transfer of the TK protein. We analyzed the presence of the TK protein in EVs by using mass spectrometry and immunoblotting and demonstrated that the TK protein can be loaded in EVs secreted from TK-containing cells.

We confirmed secretion and successful harvest of EVs in our model system according to the MISEV2018 requirements set by ISEV which demand investigation of specific proteins to evaluate the purity of the exosome isolate and other EVs [62]. Primary antibodies against calnexin, CD81, CD63, flotillin-1, TSG-101 and CD9 have already been used previously to demonstrate the presence (or absence in case of calnexin/calreticulin) of the EV-associated proteins to confirm the existence of EVs. However, the enrichment of marker proteins depends on the parental cell type and some EV markers are not always present in all EVs [88]. Our results showed that CD81 was abundant in the EVs of U87 and its derivative cells in a consistent manner and therefore we selected CD81 as a reliable EV marker protein in this study. We also showed that CD81 was enriched in P3/P3.TK, a GBM cell line cultured in serum-free medium.

Even though immunoblotting is a sensitive analysis method, we confirmed the presence of EVs with a second method. TEM analysis revealed bilayered-membrane vesicles that were cup-shaped and heterogenous in size, which is characteristic for EVs. The exosomes and MVs were found to have a size that correlates with the predicted size of the EVs in the literature [58, 63]. Electron microscopy in general (TEM or Scanning electron microscope (SEM)), is a standard method for characterizing the morphology of particles smaller than 300 nm [89]. Even though the method provides us with morphological information such as shape and size, it does not allow to fully discriminate between the vesicle subtypes but confirm the presence of the EVs. ApoBDs and MVs samples can still be contaminated with exosomes. Indeed, our TEM analysis shows that the ApoBDs may have been contaminated with other EVs. This issue could have been resolved by using specific markers found to be enriched in ApoBDs of some cell types. Example of such marker proteins are Annexin V, Thrombospondin and C3b [63] [75]. ApoBDs and MVs samples can still be contaminated with exosomes which can explain the size discrepancy observed in the images of ApoBDs. However, for precise determination, investigation with Nanoparticle Tracking Analysis (NTA) would be necessary.

Further, to investigate the effects of GCV-treatment on the EVs, we subjected the different EV fractions and cell lysates to mass spectrometric analysis. First, we identified at least 1300 different proteins with modest increase of proteins in EVs and cell lysates treated with GCV. The separate clustering of EVs and cell lysates also

confirms the diverse nature of the proteins presented in the EVs and cell lysates. We also observed that the exosomes were separately clustered in one group and the rest of the EV subtypes in another group.

Detailed analysis of the mass spectrometry data reveled an upregulation of CD81 and CD9 in these EV subtypes upon GCV treatment, suggesting that the extent of secretion of exosomes and MVs was increased following TK/GCV treatment. Immunoblot analysis showed a trend of similar increase. In line, mass spectrometry data showed that more TK and GFP protein is loaded in EVs following GCV treatment, which may also indicate the increased extent of EV secretion. In this context, it is noteworthy that immunoblot is in general not fully quantitative and thus not the best method to investigate extent of secretion of EVs. Furthermore, in our experiments, we did not use any loading controls which could be used as a normalizing factor. Recent evidence shows the presence of house keeping genes including Actin and GAPDH, but they differ in band intensity between the vesicles type [90] . Therefore, there is no specific loading control that could define as a house keeping gene for EVs. Thus, although our data indicate that TK/GCV therapy increases the secretion of exosomes and MVs, further confirmation by using quantitative nanoparticle analysis would be absolutely necessary.

After having confirmed that the HSV-TK protein is loaded as a cargo in all vesicle fractions, we wanted to determine if the TK protein has enzymatic activity following transfer into the recipient cells. As our proteomic results revealed that the ApoBDs had the highest amount of TK protein, we proceeded with this EV-subtype to analyze the suicide effect on recipient cells. We performed a cell viability assay (WST-1 assay), where we expected that the recipient naïve cells incubated with TK containing ApoBDs would have increased cell death upon treatment with GCV. However, our results did not show any suicide activity. Unfortunately, due to the crisis related to COVID-19 and consequent time restrictions, we performed this experiment only once. Thus, no major conclusion can be drawn yet. In future more experiments will be necessary to verify this observation. It would be also important to optimize the experimental protocol. For instance, in our set-up we did not centrifuge the ApoBDs after applying them onto naïve cells. Subsequent centrifuge may improve the uptake. Thus, in the future the potential uptake may be facilitated by centrifuging the plates after addition of ApoBDs in order to make sure that the ApoBDs get incorporated into

the recipient cells, and not float in the media without contact to the recipient cells. One should also include ApoBDs from U87 wild-type cells as control to get more reliable results. It would be important to analyze if the transfer is successful with ApoBDs and MVs as well.

Since exosomes and MVs from the TK positive cells also contain the TK protein it will be important to investigate the potential transfer and cytotoxicity of these fractions by using WST assay in a similar manner as for ApoBDs in future. In this regard, we have observed that the exosomes surround the nuclei of recipient cells, suggesting that the U87 cells may be susceptible for uptake of exosomes. More advanced microscopy will be needed to confirm if the vesicles are on top or inside the recipient cells.

In the future it will be important to verify all results in an additional cell line and most preferably in the P3/P3 TK cell line. The P3 cell line is a patient-derived GBM cell line cultured in serum-free media which is more relevant to the clinical scenario [91]

In the future, it will also be important to analyze if the TK mRNA can be loaded into the EVs and if so, one should investigate if this mRNA eventually can be transferred into the recipient cells and translated into protein. One possible way to analyze if the mRNA is loaded in the EVs is to perform quantitative reverse transcriptase PCR (qPCR) by using primers against the TK.GFP transgene. Furthermore, it should be investigated whether the metabolized toxic GCV-DP/TP could contribute to BE by traveling through EVs. This could be approached by mass spectrometry to reveal the abundance of GCV-DP/TP in EVs. Thereby, the abundance of GCV-DP/TP in the different EV subtypes could be determined as well and we could identify specific EV subtypes with a potentially high BE. Indeed, we planned to carry out this experiment. However, the proteomics facility at the University of Bergen has not the equipment and expertise for such analysis. We contacted the proteomics facility at the Norges teknisk-naturvitenskapelige universitet (NTNU) who could perform this analysis, but since they do not prioritize external projects, it was not possible to receive results in time.

It is noteworthy to mention that several important experiments of this thesis could not be pursued due to the Covid19-related crisis. The first major experiment or analysis that was hindered and finally cancelled by this crisis was Nanoparticle Tracking

Analysis (NTA). This method allows for determination of both size distribution and relative concentration of EVs in a sample and is the most reliable method for quantification of EVs [92]. The NTA was supposed to be performed with the help of our collaborator at the University of Gothenburg. This method would have been a key method to reliably quantify all EV fractions in most of the experiments of this thesis. Thus, many of our quantitative results, specially from the immunoblots, in this thesis need to be interpreted with caution.

Practically, we lost more than 1,5 months due to the crisis. The limited time did not allow us to perform cytotoxicity assays with exosomes and MVs, and also hindered us from pursuing further cytotoxicity experiments with ApoBDs with a modified protocol. Because of the unexpected results with the ApoBDs it was highly important for us to check transfer of ApoBDs into recipient cells. In the future this could be analyzed with two independent methods such as high-resolution microscopy and flow cytometry.

In the future it will be interesting to perform an inhibition experiment of exosomes and MVs. By inhibiting secretion of exosomes by GW4869 drug and MVs production by ROCK inhibitor it could be possible to confirm the involvement of EVs in the contribution of HSV-TK/GCV-mediated BE.

**Conclusion**

Our major finding and main observation from this thesis is the presence of the TK.GFP protein in ApoBDs, MVs and exosomes derived from TK-containing tumor cells cells. We show that the TK protein can be loaded into the EVs of U87 cells that express TK. Our data also suggest that there is an increase in EV-secretion following HSV-TK/GCV gene therapy which could, in theory, contribute to BE. However, we could not yet confirm such contribution when studying transfer with ApoBDs.

# Appendix I

**Heat Denaturation Digestion Protocol**

***Heat digestion:***

Add **10 – 20 µl buffer** and incubate at RT in Eppendorf mixer for 5 min (slow agitation).

*Reduction*

Add **2 -4 µl 100 mM DTT** to achieve a 10 mM DTT solution.

*Heat*

Heat sample for 6 min at 95C˚ in and Eppendorf mixer. Let sample cool down to room temperature.

*Alkylation*

Add **3 – 6 µl 200 mM IAA** for cystein alkylation, and incubate for 1h at RT in the dark

*(Note: Iodoacetamide is unstable and light-sensitive. Prepare solutions immediately before use and perform alkylation in the dark. If iodoacetamide is present in limiting quantities and at a slightly alkaline pH, cysteine modification will be the exclusive reaction. Excess iodoacetamide or non-buffered iodoacetamide reagent can also alkylate amines (lysine, N-termini), thioethers (methionine), imidazoles (histidine) and carboxylates (aspartate, glutamate)).*

To avoid unwanted protease alkylation, **add 0.9 – 1.8 µl 100 mM DTT**, and incubate 10 min. at room temperature.

*Buffer: 50 mM Tris/1mM $CaCl_2$: Add **0.61g Tris** (art. no. 252859, Sigma-Aldrich) and **15mg $CaCl_2$ x $2H_2O$** (art. no. 21097, Sigma-Aldrich, stabilize trypsin) to about 90ml $dH_2O$. Correct the pH to 7.8-8 with HCl and adjust the volume to 100ml. Store the solution at 4 ◦C.*

*100 mM DTT in MillQ water: Add **15.4 mg DTT** (DiThioThreitol, art. no. D-9163, Sigma-Aldrich) to 1ml $dH_2O$. (1M solution (154 mg/ml) may be aliquoted, and kept in freezer).*

*200 mM IAA in MilliQ water: Add **18.5 mg IAA** (Iodoacetamide, art. no. I-6125, Sigma Aldrich) to 0.5ml MilliQ water (must be freshly made and kept in the dark).*

**Oasis protocol (C18 cleanup)**

**General notes:** Method to de-salt and clean up sample after protein digestion from various digestion methods i.e filter aided sample preparation (FASP), in gel and in solution digestion. Some sample fractionation methods does not require C18 cleanup.

**Equipment needed:**

- Oasis 96 well cartridge plate
- 96 well waste plate
- 96 well elution plate
- Used Oasis 96 well cartridge and elution plate for balance when centrifuging.
- Appropriate centrifuge for plates
- Acetonitrile, Foric acid, Trifluoroacetic acid, MQ water.
- Pipettes

**NB!** Your sample should not be added before step 5. Make sure that the solutions you add to the cartridge flows through. If not, the cartridge could be damaged, change cartridge. If you want to measure protein concentration on Nanodrop after Oasis, make sure step 9 and 10 is done with FA and not TFA.

1. Place Oasis 96 well cartridge plate into waste plate.

2. Activate cartridges by adding 500 µL 80% ACN, 0.1% FA. 200 x g - 1 min. Discard flow trough

3. Wash cartridges by adding 500 µL 0.1% TFA. 200 x g – 1 min. Discard flow trough

4. Repeat step 3 by adding 500 µL 0.1% TFA. 200 x g – 1 min. Discard flow trough

5. Addition of 300 µL sample. 150 x g – 3 min. Discard flow trough

6. Wash by adding 500 µL 0.1% TFA. 200 x g – 1 min. Discard flow trough

7. Wash by adding 500 µL 0.1% TFA. 200 x g – 1 min. Discard flow trough

8. Wash by adding 500 µL 0.1% TFA. 200 x g – 1 min. Discard flow trough

9. Elute sample in 96 well elution plate. 100 µL 80% ACN, 0.1% FA. 200 x g – 1 min. **KEEP FLOW THROUGH**!

10. Elute sample in 96 well elution plate. 100 µL 80% ACN, 0.1% FA. 200 x g – 1 min **KEEP FLOW THROUGH**!

11. Dry the samples in SpeedVac. To speed up the process put samples in - 80˚C for 15 minutes.

12. When the samples are dried add 1% FA, 2% ACN

**NanoLC-ESI- QExcative HF mass spectrometry at PROBE**

About 0.5ug protein as tryptic peptides dissolved in 2% acetonitrile (ACN), 0.5% formic acid (FA), were injected into an Ultimate 3000 RSLC system (Thermo Scientific, Sunnyvale, California, USA) connected online to a Q-Excative HF mass spectrometer (Thermo Scientific, Bremen, Germany) equipped with EASY-spray nano-electrospray ion source source (Thermo Scientific).

**Trapping and desalting**

The sample was loaded and desalted on a pre-column (Acclaim PepMap 100, 2cm x 75µm ID nanoViper column, packed with 3µm C18 beads) at a flow rate of 5µl/min for 5 min with 0.1% TFA.

**LC RUN (195 min)**

Peptides were separated during a biphasic ACN gradient from two nanoflow UPLC pumps (flow rate of 250 nl/min) on a 25 cm analytical column (PepMap RSLC, 50cm x 75 µm ID EASY-spray column, packed with 2µm C18 beads). Solvent A and B were 0.1% FA (vol/vol) in water and 100% ACN respectively. The gradient composition was 5%B during trapping (5min) followed by 5-7%B over 0.5min, 7–22%B for the next 61.0min, 24-35%B over 23 min, and 35–90%B over 5min. Elution of very hydrophobic peptides and conditioning of the column were performed during 3 minutes isocratic elution with 90%B and 15 minutes isocratic conditioning with 5%B.

(a simplified elution gradient annotation – "Ret.time(%B)": 0(5) – 5(5) – 5.5(7) – 65(22) – 87(35) – 92(80) – 102(80) – 105(5) – 120(5)

**DDA, Q-Excative HF**

The eluting peptides from the LC-column were ionized in the electrospray and analyzed by the Q-Excative HF. The mass spectrometer was operated in the DDA-mode (data-dependent-acquisition) to automatically switch between full scan MS and MS/MS acquisition. Instrument control was through Q Excative HF Tune 2.8 and Xcalibur 3.1

Survey full scan MS spectra (from m/z 375-1500) were acquired in the Orbitrap with resolution R = 120 000 at m/z 200, automatic gain control (AGC) target of 3e6 and a

maximum injection time (IT) of 100ms. The 12 most intense eluting peptides above an intensity threshold of 50 000 counts, and charge states 2 to 6, were sequentially isolated to a target value (AGC) of 1e5 and a maximum IT of 110ms in the C-trap, and isolation width maintained at 1.6 m/z (offset of 0.3 m/z), before fragmentation in the HCD (Higher-Energy Collision Dissociation) cell. Fragmentation was performed with a normalized collision energy (NCE) of 28 %, and fragments were detected in the Orbitrap at a resolution of 15 000 at m/z 200, with first mass fixed at m/z 100. One MS/MS spectrum of a precursor mass was allowed before dynamic exclusion for 20s with "exclude isotopes" on. Lock-mass internal calibration (m/z 445.12003) was enabled.

**Ionsource parameter**

The spray and ion-source parameters were as follows. Ion spray voltage = 1800V, no sheath and auxiliary gas flow, and capillary temperature = 275 °C.

**Digestion**

*Sample dilution*

Add **55 – 110 µl buffer** (the urea concentration is now reduced to 1M).

Trypsinaddition for proteolysis

Add trypsin in amount about 50 times lower than the amount of protein in the sample. If the sample contains approx. Ex 100 µg protein, add 2µg of protease a ***0.5*** *µg/µl* . Check pH with a litmus paper. pH needs to be neutral/around 7 to 8. Incubate samples at 37 ˚C overnight (16h) on a thermo-shaker or in a heat cabinet.

***Stock of trypsin a 0.5*** *µg/µl (Promega, art. no. V 5111);*

*Dissolve one ampoule (20 µg trypsin porcine powder) in 40 µl Promega resuspension buffer (50 mM HAc).*

***To make aliquots of Trypsin Porcine a 1µg per 10µl*** *(Promega, art. no. V 5111)*
*Dissolve one ampoule (20 µg trypsin porcine powder) in 200 µl 50 mM acetic acid (resuspension buffer supplied from Promega). The trypsin concentration in this stock solution is then 0.1 µg/µl.*

*Aliquot a 10µl may be frozen at -20 ˚C for 1-2 months in aliquots. Trypsin stock solution may be diluted in buffer before use.*

**Acidification**

In this final step, acidify with 10% TFA (trifluoroacetic acid) to a 0.5-1% final concentration of TFA *(check with a litmus paper)*. Add 150-200 µl 0.1% TFA to dilute the sample to approx. 300µl. Proceed with desalting on OASIS C18, and dry in freezevac.

# Appendix II

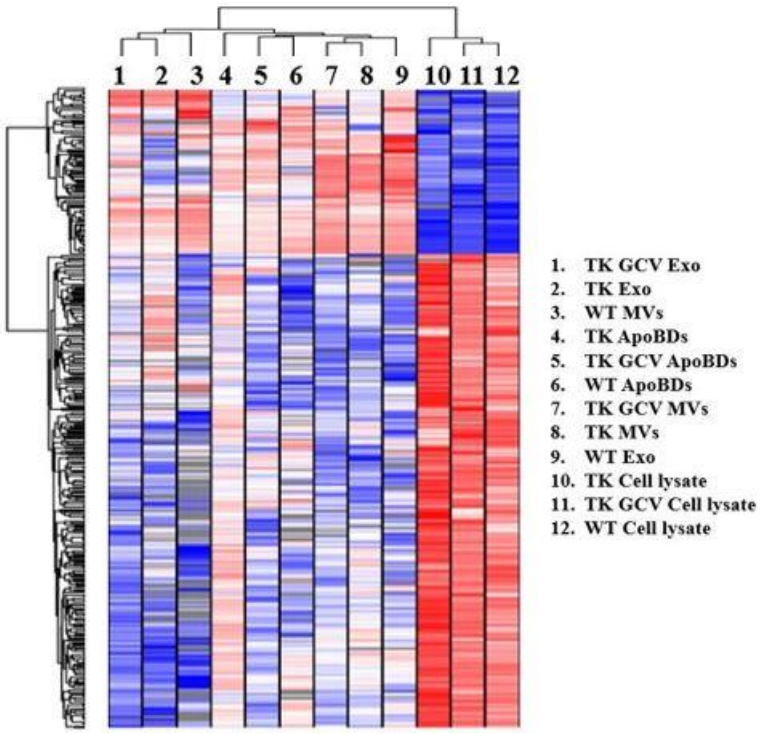


**Figure 4.10 Heatmap representing supervised clustering.** Blue represents downregulated proteins, while red represents upregulated proteins. Data represent one experiment. The samples cluster in two main groups, cell lysates and EVs.

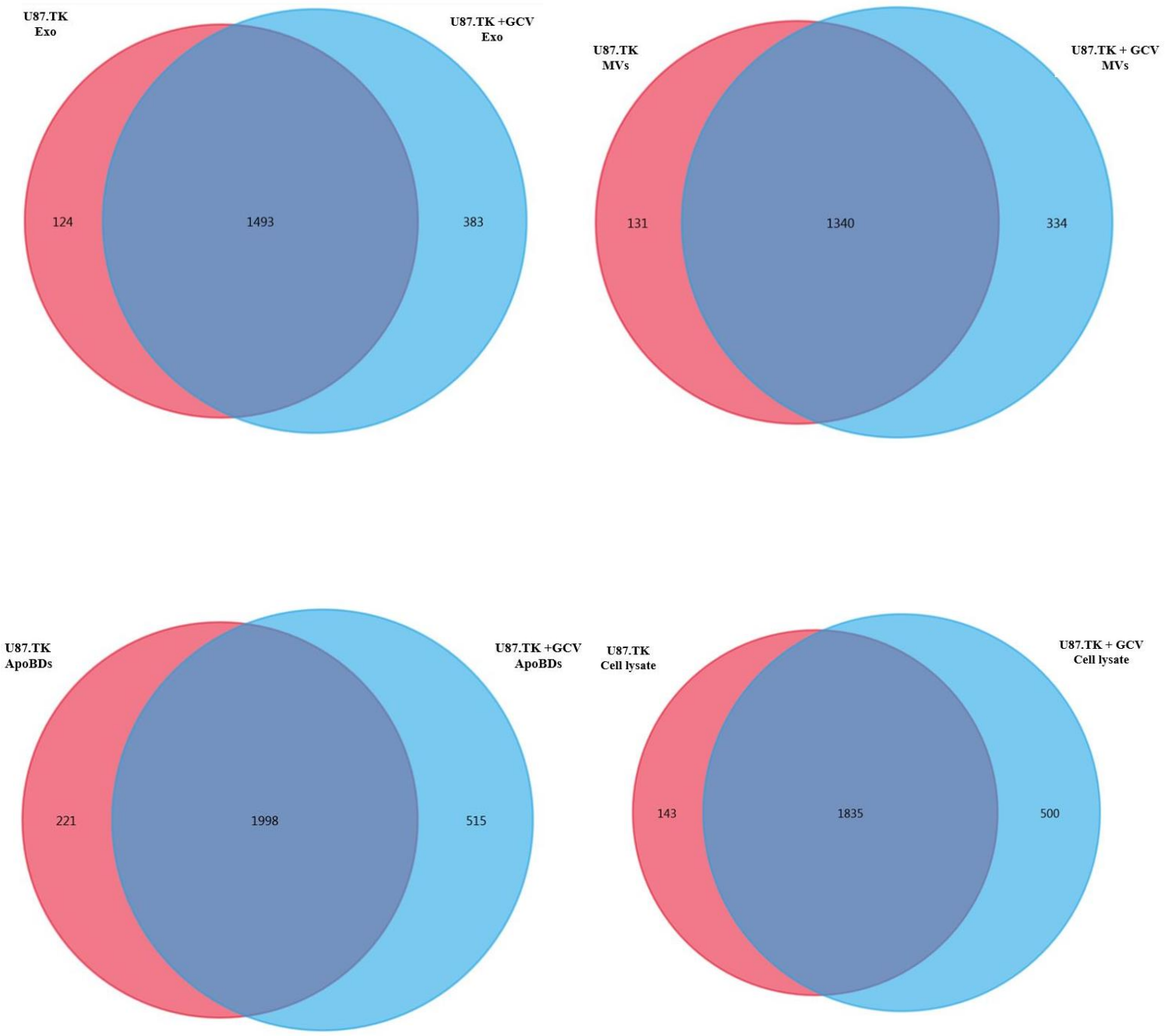


**Figure 4.11 Upregulation of proteins due to GCV-treatment.** The four venn diagrams represents the proteins found in exosomes, MVs, ApoBDS and cell lysates. We observed upregulation of proteins in GCV treated sample. This is only a trend as it represents results from only one experiment

# 7. Reference


1. GM, C., *The Development and Causes of Cancer* in *The cell: A molecular Approach* 2000, Sunderland (MA): Sinauer Associates: The National Association of Commercial Building Inspectors (NCBI)
2. Douglas Hanahan, Robert A.W., *Hallmarks of Cancer: The Next Generation*. Vol. 144. 2011.
3. Bertram, J.S., *The molecular biology of cancer*, in *Molecular Aspects of Medicine*. 2000, Elsevier.
4. Al-Dhahir., F.B.M.M.A., *Cancer, Brain Gliomas*. 2019.
5. Institute, N.C. *What is cancer* 2015 February 9; Available from: https://www.cancer.gov/about-cancer/understanding/what-is-cancer.
6. Donnola S, B.R., Hambardzumyan D, *Malignant Glioma, in Neuroglia*. 2012: Oxford Univeristy Press
7. *Network Glia*. Available from: https://www.networkglia.eu/en/classicpapers.
8. Quinn T. Ostrom, M.A., M.P.H.,1,2,* Haley Gittleman, M.S.,1,2,* Jordonna Fulop, R.N.,1 Max Liu,3 Rachel Blanda,4 Courtney Kromer, B.A.,5 Yingli Wolinsky, Ph.D., M.B.A.,1,2 Carol Kruchko, B.A.,2 and Jill S. Barnholtz-Sloan, Ph.D.1,2, *CBTRUS Statistical Report: Primary Brain and Central Nervous System Tumors Diagnosed in the United States in 2008-2012.* 2015.
9. Capper, P.W.D., *WHO 2016 Classification of gliomas*, in *Neuropathology and Applied Neurobiology* 2017. p. 139-150.
10. Kenneth D. Aldape, M.A., *Astrocytoma*. 1990, 1995, 2005, 2007, 2012, 2015: National Organization for Rare Disorders
11. MD., S.L. *Diffuse astrocytoma (grade II)*. Available from: https://braintumorcenter.ucsf.edu/condition/diffuse-astrocytoma-grade-ii.
12. Chamberlain, S.A.G.a.M.C., *Anaplastic astrocytoma.* 2016.
13. Al-Dhahir., F.B.M.M.A., *Cancer, Brain Gliomas*. Updated 2019 Dec 22: StatPearls [Internet]. Treasure Island (FL): StatPearls Publishing.
14. Kaja Urbańska, c.a.J.S., Maciej Szmidt, and Paweł Sysa, *Glioblastoma multiforme – an overview.* 2014. **18(5): 307–312.**
15. Rieske P, Z.M., Biernat W, Bartkowiak J, Zimmermann A, Liberski PP., *Atypical molecular background of glioblastoma and meningioma developed in a patient with Li-Fraumeni syndrome*, in *Journal of Neuro-Oncology*. 2005. p. 27-30.
16. Vineet Tyagi, Jason Theobald, James Barger, et al., *Traumatic brain injury and subsequent glioblastomadevelopment: Review of the literature and case reports.* 2016.
17. Anselmi, E., et al., *Post-traumatic glioma: report of two cases.* Tumori, 2006. **92**(2): p. 175-7.
18. Ohgaki, H. and P. Kleihues, *Epidemiology and etiology of gliomas.* Acta Neuropathologica, 2005. **109**(1): p. 93-108.
19. Ohgaki, H. and P. Kleihues, *The Definition of Primary and Secondary Glioblastoma.* 2013. **19**(4): p. 764-772.
20. Ohgaki, H. and P. Kleihues, *Genetic pathways to primary and secondary glioblastoma.* The American journal of pathology, 2007. **170**(5): p. 1445-1453.
21. Huang, J., et al., *Isocitrate Dehydrogenase Mutations in Glioma: From Basic Discovery to Therapeutics Development.* Frontiers in oncology, 2019. **9**: p. 506-506.

22. Tso, C.-L., et al., *Distinct Transcription Profiles of Primary and Secondary Glioblastoma Subgroups.* 2006. **66**(1): p. 159-167.
23. Behnan, J., G. Finocchiaro, and G. Hanna, *The landscape of the mesenchymal signature in brain tumours.* Brain : a journal of neurology, 2019. **142**(4): p. 847-866.
24. Noushmehr, H., et al., *Identification of a CpG island methylator phenotype that defines a distinct subgroup of glioma.* Cancer cell, 2010. **17**(5): p. 510-522.
25. Oeckinghaus, A. and S. Ghosh, *The NF-kappaB family of transcription factors and its regulation.* Cold Spring Harbor perspectives in biology, 2009. **1**(4): p. a000034-a000034.
26. Ayuso, J.M., et al., *Glioblastoma on a microfluidic chip: Generating pseudopalisades and enhancing aggressiveness through blood vessel obstruction events.* Neuro-oncology, 2017. **19**(4): p. 503-513.
27. Brat, D.J., et al., *Pseudopalisades in glioblastoma are hypoxic, express extracellular matrix proteases, and are formed by an actively migrating cell population.* Cancer Res, 2004. **64**(3): p. 920-7.
28. Eman Abdelzaher, M.D., Ph.D., *CNS tumorAstrocytic tumorsGlioblastoma multiforme, NOS.* 1 March 2012.

29. Ana Rita Monteiro 1, R.H.O., Geoffrey J. Pilkington 2 andPatrícia A. Madureira 1, *The Role of Hypoxia in Glioblastoma Invasion.* 22 November 2017.
30. Davis, M.E., *Glioblastoma: Overview of Disease and Treatment.* Clinical journal of oncology nursing, 2016. **20**(5 Suppl): p. S2-S8.
31. Rivera, M., K. Sukhdeo, and J. Yu, *Ionizing radiation in glioblastoma initiating cells.* Frontiers in oncology, 2013. **3**: p. 74-74.
32. Lee, C.Y., *Strategies of temozolomide in future glioblastoma treatment.* OncoTargets and therapy, 2017. **10**: p. 265-270.
33. Wang, T., A.J. Pickard, and J.M. Gallo, *Histone Methylation by Temozolomide; A Classic DNA Methylating Anticancer Drug.* Anticancer research, 2016. **36**(7): p. 3289-3299.
34. Roy, S., et al., *Recurrent Glioblastoma: Where we stand.* South Asian journal of cancer, 2015. **4**(4): p. 163-173.
35. Aldape, K., et al., *Challenges to curing primary brain tumours.* Nature reviews. Clinical oncology, 2019. **16**(8): p. 509-520.
36. Cai, X. and M.E. Sughrue, *Glioblastoma: new therapeutic strategies to address cellular and genomic complexity.* Oncotarget, 2017. **9**(10): p. 9540-9554.
37. Gonçalves, G.A.R. and R.d.M.A. Paiva, *Gene therapy: advances, challenges and perspectives.* Einstein (Sao Paulo, Brazil), 2017. **15**(3): p. 369-375.
38. Kwiatkowska, A., et al., *Strategies in gene therapy for glioblastoma.* Cancers, 2013. **5**(4): p. 1271-1305.
39. Caffery, B., J.S. Lee, and A.A. Alexander-Bryant, *Vectors for Glioblastoma Gene Therapy: Viral & Non-Viral Delivery Strategies.* Nanomaterials (Basel, Switzerland), 2019. **9**(1): p. 105.
40. Okura, H., C.A. Smith, and J.T. Rutka, *Gene therapy for malignant glioma.* Molecular and cellular therapies, 2014. **2**: p. 21-21.
41. Archna Panghal, H.S., SJS Flora, Saba Naqvi, *Suicide gene therapy: a promising approach towards gene delivery.* Frontiers in Nanoscience and Nanotechnology, 2018.
42. H. Chong*, A.B., S. Murphy*, A. Ruchatz*, T. Clackson†, V. Rivera†, R.G. Vile, *Suicide Gene Therapy of Cancer,* in *Molecular Therapy* 2001, Elsevier. p. 98-115.

43. Zarogoulidis, P., et al., *Suicide Gene Therapy for Cancer - Current Strategies.* Journal of genetic syndromes & gene therapy, 2013. **4**: p. 16849.
44. Springer, C.J. and I. Niculescu-Duvaz, *Prodrug-activating systems in suicide gene therapy.* The Journal of clinical investigation, 2000. **105**(9): p. 1161-1167.
45. Gentry, B.G. and J.C. Drach, *Metabolism of cyclopropavir and ganciclovir in human cytomegalovirus-infected cells.* Antimicrobial agents and chemotherapy, 2014. **58**(4): p. 2329-2333.
46. Wang, J., et al., *Herpes simplex virus thymidine kinase and ganciclovir suicide gene therapy for human pancreatic cancer.* World journal of gastroenterology, 2004. **10**(3): p. 400-403.
47. Preuß, E., et al., *Cancer suicide gene therapy with TK.007: superior killing efficiency and bystander effect.* 2011(11): p. 1113-1124.
48. Ellen Preuß, A.T., Sebastian Newrzela, Daniela Brücher, Kristoffer Weber, Ulrika Felldin, Evren Alici, Gösta Gahrton, Dorothee von Laer, M. Sirac Dilber, and Boris Fehse, *TK.007: A Novel, Codon-Optimized HSVtk(A168H) Mutant for Suicide Gene Therapy.* 2010. **21**(8).
49. Karjoo, Z., X. Chen, and A. Hatefi, *Progress and problems with the use of suicide genes for targeted cancer therapy.* Advanced drug delivery reviews, 2016. **99**(Pt A): p. 113-128.
50. Mesnil, M. and H. Yamasaki, *Bystander Effect in Herpes Simplex Virus-Thymidine Kinase/Ganciclovir Cancer Gene Therapy: Role of Gap-junctional Intercellular Communication<sup>1 </sup&gt.* Cancer Research, 2000. **60**(15): p. 3989.
51. Young Gyu Kim, W.B., 1 Estrella S. Feliciano,1 Richard R. Drake,2 and a.P.J. Stambrook, *Ganciclovir-mediated cell killing and bystander effect is enhanced in cells with two copies of the herpes simplex virus thymidine kinase gene*, in *Cancer Gene Therapy* 2000: Nature America p. 240-246.
52. McCormick, F., *Cancer gene therapy: fringe or cutting edge?* Nature Reviews Cancer, 2001. **1**(2): p. 130-141.
53. Hervé, J.-C. and M. Derangeon, *Gap-junction-mediated cell-to-cell communication.* Cell and Tissue Research, 2013. **352**(1): p. 21-31.
54. Spray, D.C., et al., *Gap junctions and Bystander Effects: Good Samaritans and executioners.* Wiley interdisciplinary reviews. Membrane transport and signaling, 2013. **2**(1): p. 1-15.
55. Perkins, G., D. Goodenough, and G. Sosinsky, *Three-dimensional structure of the gap junction connexon.* Biophysical journal, 1997. **72**(2 Pt 1): p. 533-544.
56. Scott M. Freeman, C.N.A., 3 Katharine A. Whartenby, Charles H. Packman, David S. Koeplin, and a.G.N.A. Frederick L. Moolten, *The "Bystander Effect": Tumor Regression When a Fraction of the Tumor Mass IsGenetically Modified1.* American Association for Cancer Research 1993: p. 5274-5283.

57. Altanerova, U., et al., *Prodrug suicide gene therapy for cancer targeted intracellular by mesenchymal stem cell exosomes.* 2019. **144**(4): p. 897-908.
58. Raposo, G. and W. Stoorvogel, *Extracellular vesicles: exosomes, microvesicles, and friends.* The Journal of cell biology, 2013. **200**(4): p. 373-383.
59. Zhang, H.-G. and W.E. Grizzle, *Exosomes: a novel pathway of local and distant intercellular communication that facilitates the growth and metastasis of neoplastic lesions.* The American journal of pathology, 2014. **184**(1): p. 28-41.

60. Gangoda, L., et al., *Extracellular vesicles including exosomes are mediators of signal transduction: are they protective or pathogenic?* Proteomics, 2015. **15**(2-3): p. 260-271.
61. Yekula, A., et al., *Extracellular Vesicles in Glioblastoma Tumor Microenvironment.* Frontiers in immunology, 2020. **10**: p. 3137-3137.
62. Théry, C., et al., *Minimal information for studies of extracellular vesicles 2018 (MISEV2018): a position statement of the International Society for Extracellular Vesicles and update of the MISEV2014 guidelines.* Journal of extracellular vesicles, 2018. **7**(1): p. 1535750-1535750.
63. Akers, J.C., et al., *Biogenesis of extracellular vesicles (EV): exosomes, microvesicles, retrovirus-like vesicles, and apoptotic bodies.* Journal of neuro-oncology, 2013. **113**(1): p. 1-11.
64. Jiang, L., et al., *Determining the contents and cell origins of apoptotic bodies by flow cytometry.* Scientific reports, 2017. **7**(1): p. 14444-14444.
65. abcam. *Extracellular vesicles: an introduction*. Available from: https://www.abcam.com/primary-antibodies/extracellular-vesicles-an-introduction.
66. Konoshenko, M.Y., et al., *Isolation of Extracellular Vesicles: General Methodologies and Latest Trends.* BioMed Research International, 2018. **2018**: p. 8545347.
67. Skog, J., et al., *Glioblastoma microvesicles transport RNA and proteins that promote tumour growth and provide diagnostic biomarkers.* Nature cell biology, 2008. **10**(12): p. 1470-1476.
68. Rikkert, L.G., et al., *Quality of extracellular vesicle images by transmission electron microscopy is operator and protocol dependent.* Journal of extracellular vesicles, 2019. **8**(1): p. 1555419-1555419.
69. Zaborowski, M.P., et al., *Extracellular Vesicles: Composition, Biological Relevance, and Methods of Study.* BioScience, 2015. **65**(8): p. 783-797.
70. Doyle, L.M. and M.Z. Wang, *Overview of Extracellular Vesicles, Their Origin, Composition, Purpose, and Methods for Exosome Isolation and Analysis.* Cells, 2019. **8**(7): p. 727.
71. Witwer, K.W., et al., *Standardization of sample collection, isolation and analysis methods in extracellular vesicle research.* Journal of extracellular vesicles, 2013. **2**: p. 10.3402/jev.v2i0.20360.
72. Tauro, B.J., et al., *Two distinct populations of exosomes are released from LIM1863 colon carcinoma cell-derived organoids.* Molecular & cellular proteomics : MCP, 2013. **12**(3): p. 587-598.
73. Crescitelli, R., et al., *Distinct RNA profiles in subpopulations of extracellular vesicles: apoptotic bodies, microvesicles and exosomes.* Journal of extracellular vesicles, 2013. **2**: p. 10.3402/jev.v2i0.20677.
74. Heijnen, H.F., et al., *Activated platelets release two types of membrane vesicles: microvesicles by surface shedding and exosomes derived from exocytosis of multivesicular bodies and alpha-granules.* Blood, 1999. **94**(11): p. 3791-9.
75. Théry, C., et al., *Proteomic Analysis of Dendritic Cell-Derived Exosomes: A Secreted Subcellular Compartment Distinct from Apoptotic Vesicles.* The Journal of Immunology, 2001. **166**(12): p. 7309.
76. Aldrich, S. *Product Information* Available from: https://www.sigmaaldrich.com/content/dam/sigma-aldrich/docs/Sigma/Product_Information_Sheet/2/g2536pis.pdf.
77. Hossain, J.A., et al., *Long-term treatment with valganciclovir improves lentiviral suicide gene therapy of glioblastoma.* Neuro Oncol, 2019. **21**(7): p. 890-900.

78. *Counting cells using a hemocytometer*. Available from: https://www.abcam.com/protocols/counting-cells-using-a-haemocytometer.
79. *NuPAGE®Technical GuideGeneral information and protocols for using the NuPAGE® electrophoresis system*. 2010; Available from: http://tools.thermofisher.com/content/sfs/manuals/nupage_tech_man.pdf.

80. mySCOPE. *Background information - What is transmission electron microscopy?* ; Available from: https://myscope.training/legacy/tem/background/#toggleMenu.
81. *Formvar/Carbon film on Gold 200 mesh*. Available from: https://emresolutions.com/product/formvarcarbon-film-on-gold-200-mesh-25/.
82. *Microscopy Techniques and Culture Surfaces:Find the Perfect Match*. Available from: https://ibidi.com/content/216-confocal-microscopy.

83. *STED Nanoscopes Leica TCS SP8 STED*. Available from: https://www.leica-microsystems.com/products/confocal-microscopes/p/leica-tcs-sp8-sted-one/.
84. Aldrich, S. *Cell Proliferation Reagent WST-1*. 2011; Available from: https://www.sigmaaldrich.com/catalog/product/roche/cellproro?lang=en&region=NO.
85. Oh, S.-J., et al., *Human U87 glioblastoma cells with stemness features display enhanced sensitivity to natural killer cell cytotoxicity through altered expression of NKG2D ligand.* Cancer cell international, 2017. **17**: p. 22-22.
86. Sagini, K., et al., *Extracellular Vesicles as Conveyors of Membrane-Derived Bioactive Lipids in Immune System.* International journal of molecular sciences, 2018. **19**(4): p. 1227.
87. Lunavat, T.R., et al., *Small RNA deep sequencing discriminates subsets of extracellular vesicles released by melanoma cells--Evidence of unique microRNA cargos.* RNA biology, 2015. **12**(8): p. 810-823.
88. Yoshioka, Y., et al., *Comparative marker analysis of extracellular vesicles in different human cancer types.* Journal of extracellular vesicles, 2013. **2**: p. 10.3402/jev.v2i0.20424.
89. Wu, Y., W. Deng, and D.J. Klinke, 2nd, *Exosomes: improved methods to characterize their morphology, RNA content, and surface protein biomarkers.* The Analyst, 2015. **140**(19): p. 6631-6642.
90. Hu, Y., et al., *Human umbilical cord mesenchymal stromal cells-derived extracellular vesicles exert potent bone protective effects by CLEC11A-mediated regulation of bone metabolism.* Theranostics, 2020. **10**(5): p. 2293-2308.
91. Huszthy, P.C., et al., *In vivo models of primary brain tumors: pitfalls and perspectives.* Neuro-oncology, 2012. **14**(8): p. 979-993.
92. Soo, C.Y., et al., *Nanoparticle tracking analysis monitors microvesicle and exosome secretion from immune cells.* Immunology, 2012. **136**(2): p. 192-197.